Deep Learning-Based Image-to-SMILES Conversion of 2D Chemical Structures

by

ALISHA

Under the supervision

of

Dr N Arul Murugan

Indraprastha Institute of Information Technology, Delhi

July, 2025

Deep Learning-Based Image-to-SMILES Conversion of 2D Chemical Structures

by

ALISHA

Submitted

in partial fulfilment of the requirements for the degree of

Master of Technology

to

Indraprastha Institute of Information Technology, Delhi

July, 2025

Certificate

This is to certify that the thesis titled "**Deep Learning-Based Image-to-SMILES Conversion of 2D Chemical Structures**" being submitted by **Alisha** to the Indraprastha Institute of Information Technology Delhi for the award of the Master of Technology is an original research work carried out by her under my supervision. In my opinion, the thesis has reached the standards fulfilling the requirements of the regulations relating to the degree. The results contained in this thesis have not been submitted in part or full to any other university or institute for the award of any degree/diploma

July , 2025

Dr. N Arul Murugan
Department of Computational Biology
Indraprastha Institute of Information Technology
Delhi, New Delhi 110020

Acknowledgements

I am sincerely grateful to Dr. N. Arul Murugan, my thesis supervisor, for their invaluable mentorship and unwavering support throughout this endeavor. His expertise and encouragement played a pivotal role in the successful completion of this thesis.

I am also indebted to all the faculty and staff at IIIT Delhi for their consistent assistance, which greatly facilitated the entire process. Thank you all for your guidance and support. I am indebted to my fellow batchmates for their encouragement and support.

Lastly, heartfelt thanks are extended to my family and friends, whose enduring support and inspiration have been pivotal throughout my academic journey. Their unwavering confidence in me has made this achievement possible.

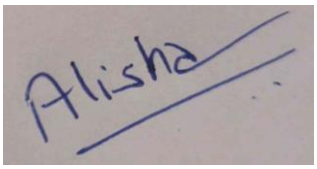

ALISHA
(MT23240)

Abstract

Chemical information science faces an important bottleneck because millions of chemical structures are trapped in visual formats throughout scientific literature and patents, making them inaccessible for automatic analysis and large-scale data mining. Traditional optical chemical structure recognition (OCSR) methods depend on the rules-based approaches that demonstrate limited robustness when processing the real-world literature diversity, while the current deep learning approaches seek large-scale computational resources yet remain impractical for comprehensive deployment.

This research addresses these limitations through the development of an integrated three-phase deep learning pipeline that (1) a Faster R-CNN with ResNet-50 backbone and Feature Pyramid Network architecture adapted for chemical structure detection, handling diverse molecular configurations across 15 chemical elements and 4 bond types (19 classes total); (2) uses spatial connectivity analysis using K-D tree algorithms to generate adjacency and bond-order matrices for molecular graph representation; and (3) uses multi-strategy SMILES generation with progressive RDKit sanitization, fragment-linking, and domain-aware validation. Key technical innovations include chemical-aware anchor generation, class-specific confidence thresholds, focal loss implementation, and strategic training methodologies addressing severe class imbalance.

The developed system displays strong performance through comprehensive evaluation on 14,997 testing images; 612,371 total detections (99.7% detection rate) at 40.83 detections per image, 99.2% successful molecular graph conversion, 98.1% right bond connectivity, and SMILES generating (41.2% valid). While 25 epochs on the full 100K dataset are converged to a loss of 0.8877. The system achieves an mAP of 74.9% with 88.1% of successfully generated molecules that receive high-quality scores (80) on the comprehensive verification metrics. The framework is optimized for standard computational infrastructure with efficient memory use.

Contents

Chapter 4

4. Materials and Methods
    4.1. System Setup and Environment
        4.1.1. Software Environment and Framework Configuration
    4.2. Hardware Configuration and Computational Resources
    4.3. Dataset Composition and Preparation
        4.3.1. Chemical Structure Image Dataset
    4.4. Annotation Structure and Class Definition
        4.4.1. Data Preprocessing and Partitioning
    4.5. Model Architecture and Training
        4.5.1. Faster R-CNN Architecture with Chemical Optimization
        4.5.2. Progressive Training Methodology
        4.5.3. Optimization Strategies and Efficiency Measures
    4.6. Inference and Processing Pipeline
        4.6.1. Object Detection and Localization
        4.6.2. Spatial Relationship Analysis
        4.6.3. Molecular Graph Construction
    4.7. SMILES Generation and Validation
        4.7.1. RDKit Integration and Molecular Processing
        4.7.2. Multi-Strategy SMILES Generation Framework
    4.8. Evaluation Framework
        4.8.1. Performance Assessment Methodology
    4.9. Validation and Quality Assessment
    4.10. System Integration and Deployment

Chapter 5

5. Experimental Framework
    5.1. Deep Learning Model for Chemical Structure Detection
        5.1.1. Introduction to Chemical Structure Object Detection
        5.1.2. Chemical-Specific Detection Challenges
    5.2. Faster R-CNN Architecture Implementation
        5.2.1. Framework Overview and Two-Stage Detection
        5.2.2. ResNet-50 backbone Architecture
        5.2.3. Feature Pyramid Network Integration
    5.3. Dataset Utilization and Training Strategy
        5.3.1. Comprehensive Dataset Composition
    5.4. Strategic Subset Training Methodology
    5.5. Model Architecture and Optimization
        5.5.1. Optimized Architecture Configuration
        5.5.2. Progressive Training and Optimization Strategies

Chapter 7

Chapter 8

8. Discussion and Impact Analysis
    - 8.1. Performance Evaluation and Technical Achievements
    - 8.2. Technical Innovation and Methodological Contributions
    - 8.3. Applications and Broader Impact
    - 8.4. Current Limitations and Future Development Opportunities

Chapter 9

9. Conclusion and Future Work
    - 9.1. Research Accomplishments and System Performance
    - 9.2. Technical Innovation and Methodological Contributions
    - 9.3. Current Limitations and Future Development Opportunities
    - 9.4. Future Research and Development Pathways

References

List of Figures

Figure 16: IoU threshold analysis displaying precision, recall, F1-score, and mAP performance across intersection-over-union thresholds for spatial accuracy assessment

Figure 17: Class-specific performance analysis showing precision, recall, F1-score, and average precision for all 19 chemical classes with detailed performance metrics per element and bond type

Figure 18: Detection visualization example showing complex molecular structure with color-coded chemical element identification and confidence scores overlaid on original image

Figure 19: Overall system performance summary showing key metrics including total images tested, detection rate, average detections per image, and confidence statistics

Figure 20: Raw detection JSON format showing structured output with atoms and connections including bounding boxes, confidence scores, and chemical classifications

Figure 21: Molecular graph visualization showing detected structure with corresponding node-edge network representation for pharmaceutical compound analysis

Figure 22: Adjacency and bond-order matrices showing mathematical representation of molecular topology with connectivity patterns and bond type encoding

Figure 23: SMILES generation examples showing diverse molecular structures with corresponding canonical notation demonstrating chemical representation capabilities

Chapter 1

1. Introduction

1.1. The Critical Challenge of Chemical Information Extraction

The exponential growth of chemical literature represents both an unprecedented opportunity and a malignant challenge for computational chemistry. Countless chemical structures are embedded within chemical compounds and scientific publications documented in databases such as PubChem. Access to chemical information has become an major bottleneck in modern research and development. Published chemical structures are causing a significant obstacle to mining and systematic analysis of chemical knowledge.

Drug patents have thousands of molecular structures per document, while individual research articles usually have many different chemical structures. Each structure carries valuable information about molecular properties, synthetic routes, and biological activities that are largely inaccessible for computational analysis. This trapped information represents a significant loss of scientific capital and limits our ability to discover chemical data mining, structural relationship analysis, and automatic chemical knowledge.

1.2. Historical Development of Chemical Structure Recognition

The pursuit of automatic chemical structure recognition has developed through different technical stages, each new challenge addressing specific limitations. The initial approach depended on the rule-based systems, which employed geometric heuristics and pattern-matching heuristics to identify chemical elements and bonds within document images. These systems performed fundamental brittleness when these systems were faced with real-world literature diversity, drawing convention diversity, and image quality decline.

The introduction of optical character recognition (OCR) technologies provided initial capabilities to extract text chemical information but failed to address the spatial relationships and connectivity patterns required for molecular structure interpretation. The specific chemical OCR system emerged in the 1990s, which included domain-specific knowledge about chemical structural conventions but was limited by its dependence on high-quality images and standardized drawing conventions.

The arrival of machine learning techniques introduced new possibilities for chemical structure recognition through pattern learning rather than rule specification. Support vector machines, random forests, and other classical machine learning approaches enable stronger handling of image variations and drawing styles. However, these methods required extensive feature engineering and remained constrained by the complexity of chemical structure representation.(Mater & Coote, 2019)

.

1.3. Deep Learning Models in Atom and Bond Detection

The deep learning revolution has fundamentally changed chemical structure recognition capabilities. Convolutional neural networks (CNNs) enable automatic feature extraction from chemical composition images, while attention mechanisms and transformer architecture provide sophisticated spatial relationship

modeling. Recent progress in the object detection architecture, including R-CNN variants and YOLO implementation, has enabled simultaneous identification and classification of many chemical elements within complex molecular diagrams. Deep learning models have revolutionized atoms and bonds through their ability to directly learn complex spatial ties and chemical patterns directly from training data. Convolutional neural networks excel at extracting hierarchical features from chemical structure images, progressing from low-level edge detection and texture analysis to high-level pattern recognition of specific atomic elements and relationship systems.(Rajan et al., 2021)

The success of deep education in chemical structure recognition stems from many major architectural innovations. ResNets enable very deep architecture training that can catch complex chemical relations while avoiding the vanishing-gradient problem. Skip connections in ResNet architecture allow information flow on several parameters, which enables both local nuclear details and recognition of global molecular patterns. The attention mechanism provides additional sophistication for chemical structure recognition by enabling the model to focus on relevant spatial regions while suppressing the intervention of the background. The self-attention mechanism allows the model to establish long-distance dependence among distant molecular components, which is particularly important for identifying cyclic structures and extended conjugated systems where nuclear interactions spread to a large spatial distance.

Transfer learning strategies have proved particularly valuable for chemical composition recognition applications where label training data may be limited. Fine-tuned for chemical data developed on large-scale image datasets, they provide strong feature extractors that may be fine for chemical-specific recognition functions. This approach enables effective training on small chemical composition datasets, taking advantage of general visual pattern recognition capabilities.(Yoshikai et al., 2024)

1.4. Object Detection in Chemical Structure Recognition

Object detection represents an important technical component in modern chemical composition recognition systems, providing the foundation to identify and localize individual atoms, bonds, and functional groups within molecular diagrams. Unlike traditional image classification models, which assign a single label for complete images, object-detection models must simultaneously localize and classify several objects within spatial contexts, especially suitable for chemical composition analysis where individual molecular components should be identified and their relationships should be preserved.

Contemporary object detection architecture employs refined feature extraction and spatial analysis techniques that are well aligned with chemical composition recognition requirements. Region-based CNN (R-CNN) architecture, including Fast R-CNN and Faster R-CNN implementation, provides strong structures to detect chemical elements with individual scales and geometric arrangements. This architecture generates the resolution of the area for potential items, extracts features using CNN backbones, and classifies areas by refining localization through the bounding box region.(Redmon et al., 2016)

The paradigms to detect two-stage pipelines of R-CNN variants provide special benefits for chemical composition recognition. The initial area proposal for the phase enables efficient handling of complex molecular arrangements where chemical elements may appear in diverse scales and tilts. The latter classification and the refinement phase allow for accurate localization of atomic positions and bond connectivity, which is essential for accurate molecular graph construction and SMILES production.

Feature Pyramid Network (FPN) chemical composition represents another significant advancement for recognition applications. Both FPN architectures enable both fine details, such as nuclear symbols and electron arrangements, and the effective structural patterns, including the ring system and molecular structure. This multi-level capacity is essential for chemical composition recognition where molecular complexity spreads several spatial parameters within individual images.

1.5. SMILES: The Foundation of Chemical Informatics

The simplified molecular input line entry system (SMILES) represents one of the most important progressions in chemical informatics, which provides a standardized method to represent molecular structures as ASCII strings. Developed by David Venninger in the late 1980s, SMILES notation enables efficient storage, transmission, and computational manipulation of chemical structures without the complications of graphical representation. The system encodes molecular connectivity, stereochemistry, and electronic properties in a compact, machine-readable format that has become a de facto standard in computer chemistry applications (Figure 1).

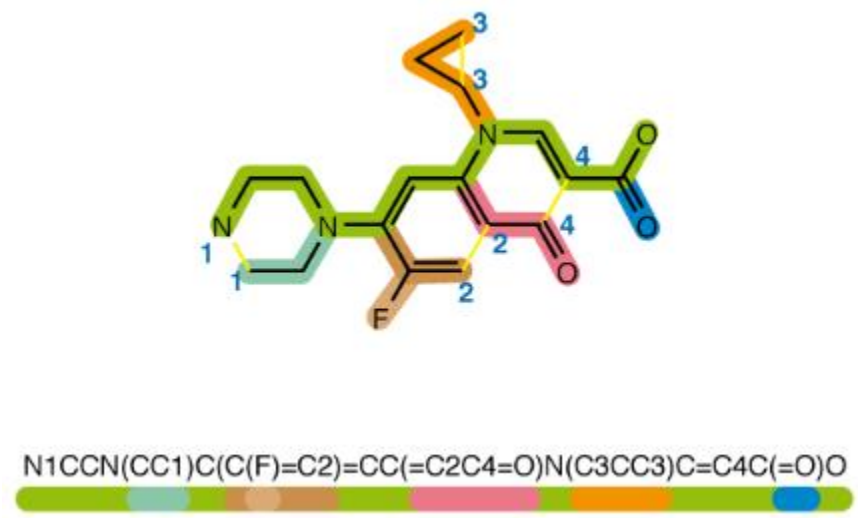

Figure 1: Example of chemical structure recognition showing molecular diagram and corresponding SMILES notation(Sella, n.d.)

The importance of SMILES notation is much higher than simple data storage. SMILES strings enable rapid molecular equality discovery, substructure analysis, and the prediction of the property through the cheminformatics algorithms. Major chemical databases, including ChEMBL, PubChem, and ZINC, rely on SMILES notation for composition sequencing and recovering. In addition, drug discovery, materials science, and synthetic chemistry all rely on rapid feature extraction and SMILES representations in ML workflows. for future modeling.

The development of SMILES notation has progressed in computational chemistry and data science. The original SMILES specifications focused on basic connectivity representation, while later development introduced a canonical SMILES for unique molecular representation, isomeric SMILES for stereochemical specifications, and reaction SMILES for chemical changes encoding. Recent extensions include smarter

pattern matching and smarts for various machine learning-optimized representatives that facilitate deep learning applications in chemical space exploration.

The integration of domain-specific knowledge in deep learning architecture represents an active field of research and development. Data-augmentation strategies, loss functions that penalize chemically invalid outputs, and post-processing algorithms that ensure molecular graph stability all contribute to better recognition accuracy and chemical validity of the results generated.

The modern chemical structure recognition system displays successful integration of these deep learning advances with domain-specific chemical knowledge. The combination of a strong object detection framework, sophisticated neural architectures, and chemical verification procedures enables automated extraction of molecular information from diverse literature sources with the level of accuracy for production in chemical informatics applications.

Chapter 2

2. Advanced Chemical Structure Recognition—An Optimized Deep Learning Approach

2.1. Research Foundation and Problem Definition

2.1.1. The Chemical Information Processing Challenge

Contemporary chemical research encounters an important information processing bottleneck that affects the entire discipline. Digital chemical databases such as PubChem have experienced dramatic expansion, now having more than 100 million compounds, yet most chemical knowledge remains trapped within visual formats throughout scientific literature (Filippov & Nicklaus, 2009). This creates a fundamental access problem that disrupts large-scale chemical knowledge extraction and computational analysis in research publications. Research publications regularly occur with between 15 and 50 separate chemical structures per article, while pharmaceutical patents contain thousands of molecular representations within single documents. The visual embedding of this chemical information creates systematic obstacles for automatic analysis and prevents researchers from accessing collective chemical knowledge contained within scientific literature efficiently.

The challenge extends beyond simple data extraction due to the wide variety of chemical structure representation methods. Chemical structures appear in various visual formats, including hand-prepared skeletal formulas and computer-generated molecular diagrams. Each representation employs distinct conventions for stereochemistry, bond notation, and atomic-labeling systems. Historical documents introduce additional complexity through obsolete marking systems and image degradation during digitization. This representative diversity requires strong recognition systems capable of processing various drawing styles while maintaining chemical accuracy(Rajan et al., 2020). The current optical chemical structure recognition (OCSR) system displays sufficient limitations that prevent widespread implementation in the production chemical information science environment. The comprehensive evaluation of existing approaches exhibits the shortcomings of systematic shortcomings on key benchmarks. Traditional rule-based systems show severe brittleness when processing the real-world chemical literature diversity, while contemporary deep learning approaches demand large-scale computational resources and training on over 400 million images to achieve competitive performances on standardized benchmarks(Oldenhof et al., 2020).

2.1.2. Strategic Research Objectives and Technical Framework

This research addresses these boundaries through the development of a customized deep learning method that achieves production-grade performance using intelligent training strategies and architectural adaptation. Rather than brute-force training on massive datasets, we use strategically curated samples. The task presents a systematic approach that achieves extraordinary performance using strategically curated data extracted from a broad chemical structure collection.

The technical framework addresses three important areas where existing approaches display systematic boundaries. First, the object detection architecture designed for natural images fails to customize the anchor generation and feature extraction strategies for specific geometric features of chemical structures (Lin et al., 2017). Second, post-processing techniques to refine raw detections of raw detection for chemically valid

molecular illustrations remain underdeveloped and inadequate across diverse structure types. Third, extensive extensivevalidation framework are largely absent from current research literature to assess the practical usefulness of chemical accuracy and generated SMILES representations.

2.2. Core Technical Methodologies and System Architecture

2.2.1. Strategic Dataset Optimization and Training Methodology

We employ a customized training pipeline—combining smart model selection with progressive fine-tuning—to achieve strong performance. The functioning of the 10,000-image subset extracted from a comprehensive 100,000-image collection is carefully curated, reaching high performance levels and achieving convergence in just 37.2 minutes of training in 6 epochs.

This strategy offers several practical benefits, including an accelerated development cycle, low computational requirements, and increased model capacity. This custom subset maintains representative coverage in all major chemical structure types, enabling rapid use and parameter optimization. This approach displays effective training progression, with the detection rate improving from 9.18 to 33.42 objects per image in training periods, representing a 264% improvement in molecular structure recognition capacity.

Customized training configurations include several technical enhancements. Mixed-precision training provides improvement in adequate computational efficiency while maintaining numerical stability, which enables a large effective batch size within the GPU memory constraints by reducing training time by about 40%. Gradient accumulation yields an effective batch size of 16, enabling stable training under memory limits with available computational resources and provides stable training dynamics adapting memory usage.

2.2.2. Specialized Detection Architecture for Chemical Structures

The main technical contribution involves the development of a novel architecture adapted to the chemical composition recognition challenges, especially for chemical structure recognition challenges. This architecture covers domain-specific knowledge about chemical composition characteristics while maintaining suitable computational efficiency for mass deployment applications. Architectural adaptation centers on special anchors whose aspect ratios and scales are tailored to common bond lengths and atom sizes about specific molecular geometry, scale distribution, and spatial relationships. Unlike normal object detection approaches, which employ standard anchor patterns, this special architecture produces tuners specifically for chemical composition characteristics, including general aspect ratio, scale variation, and geometric arrangements in molecular diagrams(Lin et al., 2017).

Multi-scale feature processing capabilities enable simultaneous structural patterns, including ring systems and molecular structures, as well as simultaneous accreditation of fine-and-corrections, such as nuclear symbols and bond stereochemistry. Architecture incorporates special FPN, enabling effective processing of chemical structures spread in diverse spaces by individual images. The chemistry-informed spatial analysis implementation uses sophisticated geometric algorithms, which determine tolerance to uncertainties with efficient proximity analysis and tolerance for connectivity determination, including KD-trees for nearest-neighbor bond-atom matching. These algorithms integrate chemical knowledge about vague bond length, angle, and connectivity patterns to guide the molecular graph construction while handling the ambiguous identity results.

2.3. Key Chemical Informatics Concepts and Validation Framework

2.3.1. Molecular Graph Theory and Chemical Representation

The molecular graph theory provides a mathematical foundation for representing chemical structures in computational systems. In this structure, atoms are represented as nodes , while chemical bonds form the edges connecting these corners. This graph-theoretic representation enables systematic analysis of molecular connectivity, stereochemistry, and chemical properties through well-established mathematical algorithms(Todeschini & Consonni, 2009).

The molecular graph construction process involves converting the consequences of raw identification from computer vision algorithms into chemically meaningful graph structures. This change requires sophisticated spatial analysis to determine the connectivity between the atoms detected during accounting to detect uncertainty and various drawing conventions. The resulting molecular illustration should satisfy fundamental chemical principles, including valence constraints and connectivity rules(Fang et al., 2023).

Chemical verification structures ensure that molecular graphs generated represent chemically viable structures. These verification systems include specific bond lengths, angles, and comprehensive chemical knowledge, including the connectivity pattern. Automatic improvement capabilities address general identity errors while maintaining the chemical validity of molecular representations.

2.3.2. SMILES notation and Chemical Database Integration

The simplified molecular input line entry system (SMILES) serves as a standard signaling to represent molecular structures as ASCII strings(Weininger, 1988). SMILES notation enables efficient storage, transmission, and computational manipulation of chemical structures without the need for graphical representation. This linear notation system encodes molecular connectivity, stereochemistry, and electronic properties in a compact, machine-readable format.

The SMILES-generation module represents a significant final stage in converting standardized molecular illustrations for humanized chemical representation suitable for integration and computational analysis. The conversion process should preserve molecular properties and structural information by ensuring syntactic purity according to SMILES specification standards.

The quality-evaluation framework assesses each SMILES string in several supplementary criteria to ensure chemical accuracy and practical utility. Syntactic verification confirms that all generated SMILES conform to standard syntax requirements that enable passing through cheminformatics software. Semantic verification preserves molecular properties using molecular descriptors (e.g., molecular weight, logP) and connectivity patterns during recognition and generation processes (Landrum, 2023).

2.3.3. Optical Chemical Structure Recognition (OCSR) and Performance Evaluation

optical chemical-structure recognition (OCSR) incorporates a full pipeline to extract chemical composition information from visual representation. The process includes image preprocessing, detection of chemical elements, bond identity, molecular graph construction, and SMILE generation, including many sequential stages(Staker et al., 2022). Each stage introduces potential error sources that can deposit and affect the

final output quality.Performance evaluation for the OCSR system requires comprehensive evaluation across multiple metrics. The accuracy of detection measures the ability of the system to correctly identify and detect chemical elements within the input images. Graph-reconstruction accuracy measures the conversion of raw detection for meaningful connectivity representation. Smiles generation quality downstream assesses the chemical validity and practical utility of the final output for the applications (Kohulan et al., 2022). The round-trip verification provides a significant quality assurance mechanism by comparing the generated SMILES to the original structures via a round-trip conversion in molecular representations. This verification approach ensures complete recognition and structural protection during the generation process, identifying systematic error patterns that may require targeted improvements.

2.4. Performance Results and System Validation

2.4.1. Detection Performance and Chemical Element Recognition

Customized system comprehensive evaluation achieves high performance levels in the dataset. The testing on 14,997 images demonstrates robust structure recognition with reliable performance in diverse molecular types and complexity levels. The primary performance metrics display strong capacity: a 99.7% detection rate in testing images with successful chemical element detection, an average of 40.83 detections per image providing wide molecular structure coverage, and a mean confidence score of 0.741 indicating reliable detection. The system produced 612,371 total chemical detections, which demonstrate extensive chemical entities in diverse molecular types.

Element-wise breakdown shows coverage across pharmaceutical and materials-chemistry applications. Carbon detection gained 200,129 successful identifications by demonstrating strong organic chemistry coverage. Single bond detection reached 225,085 instances, enabling accurate molecular connectivity analysis, while the detection of the aromatic system attained 116,786 examples, supporting complex ring structure analysis. The detection of special elements includes 28,810 oxygen detections, 17,433 nitrogen detections, and broad heteroatom coverage with halogen detection, including 4,074 chlorine, 589 bromine, 389 fluorine, and 32 iodine instances. The system displays capacity for special elements, including 837 phosphorus and 2,363 sulfur detections, supporting various chemical applications.

2.4.2. Molecular Graph Construction and SMILES Generation

The molecular-graph construction pipeline converts raw detections into chemically meaningful graphs with a high success rate. Graph construction succeeds in 99.2% of images where atoms were detected (14,884/14,997) and achieves 98.1% bond-connection success (14,715/14,997).

The performance analysis of the SMILES generation shows that the 14,884 total generation efforts are successfully processed by molecular illustration, representing a 41.2% success rate with 6,127 valid SMILES. The system produced 5,341 unique molecular instances, showing a suitable chemical variety for database applications. High-quality molecule generations achieved 5,399 structures (e.g. QED score ≥ 0.80), while the

average quality score reached 86.6%, indicating strong chemical validity for successively generated structures (Bickerton et al., 2012).

Round-trip verification displays high reliability with a 96.2% success rate for structure preservation when generated, which smiles back in molecular representations and compares with original structures. Chemical diversity analysis reveals adequate molecular diversity, supporting diverse organic chemical families with wide element distribution with 12 separate chemical elements, supporting diverse chemical information science applications.

Chapter 3

3. Literature Review and Methodological Foundations

3.1. Evolution of Chemical Structure Recognition Systems

3.1.1. Early Computational Approaches

When applied to chemical diagrams, the development of automatic chemical structure recognition emerged from the boundaries of traditional optical character recognition. In 1992, the basic work of McDaniel and Balamath established the conceptual framework, which disintegrated the chemical structure recognition in the discrete processing stages: image preprocessing, symbol identification, bond detection and molecular reconstruction(McDaniel & Balmuth, 1992). Early commercial systems, including Kekulé and CLiDE, represented early efforts to address this challenge through rules-based approaches, which encoded chemical knowledge about specific bond lengths, atomic arrangements, and spatial relations.

These early systems achieved proper performance on standardized chemical paintings, but performed fundamental boundaries when faced with diverse drawing styles and image quality variations found in real -world literature. Strict rules and based structures failed when facing unusual drawing conferences, diverse line thickness, or non-standard fonts. Analysis of historical chemical literature reveals the continuous development of drawing traditions in decades, causing variations that challenge predetermined views of constant visual appearance.

The advent of statistical learning methods in the late 1990s and early 2000s addressed the rules-based limitations through machine learning techniques, which were adapted to various input characteristics through training rather than manual programming. Support vector machines emerge as emerged as especially effective for chemical element classification, perform better strength than rigid rules-based approaches. In this period, fundamental ideological changes were observed from classification to generation, composition recognition was considered as translation from view to text representation rather than static classification.

3.1.2. Contemporary Deep Learning Architectures

The emergence of deep learning basically changed chemical structure recognition by enabling the end-to-end learning to chemical representations from the images.DECIMER system introduced by Rajan et al. , DECIMER's Show-and-Tell neural network treated the recognition of chemical composition as image captioning with chemical structures, using deep neural network for visual feature extraction and recurrent neural network for sequential SMILES generation(Rajan et al., 2021).

DECIMER training method depends on the synthetic dataset generation, making more than 400 million chemical composition images from the molecular database. This huge scale addressed the lack of training data, enabling systematic coverage of chemical space diversity. However, this approach created adequate computational requirements and potential domain adaptation challenges when applying trained models in real -world literature with various visual features. The performance assessment demonstrated 73.25% accuracy on hand-designed structures, representing sufficient progress on earlier approaches, revealing significant intervals for production applications requiring high reliability(Rajan et al., 2021).

Alternative architectural paradigms have detected different approaches for chemical composition recognition. The MolScribe system performed competitively with a fairly small training dataset (for DECIMER, 400+ million vs. 400+ million), suggesting that architectural efficiency partially compensates for training data limitations(Qian et al., 2023). The IMG2MOL framework emphasized computational efficiency through a combination of pre-educated CNN encoders with special chemical decoders, indicating that transfer from general computer vision functions can provide effective convenience representations for transfer chemical applications(Clevert et al., 2021).

3.2. Object Detection Advances and Chemical Applications

3.2.1. Evolution of Detection Architectures

The object detection architecture has progressed from general-purpose systems for natural images to specialized architectures to address the unique features of the technical domain. The detection of the chemical structures presents special challenges, including extreme aspect ratio variation, accurate geometric relationships, and element distribution across multiple scales. The R-CNN family development reflects systematic improvement in both accuracy and computational efficiency through architectural innovations (Girshick et al., 2014).

Processing ~2,000 region proposals per image of the original R-CNN created computational hurdles independently that hinder practical deployment. Fast R-CNN addressed these limitations through feature sharing and ROI pooling, while Faster R-CNN ended the dependence on the external area proposal methods through the Region Proposal Network (RPN). Feature Pyramid Network enhances a multi-scale object detection capacity by creating a feature hierarchy that preserves both spatial resolution and semantic information (Lin et al., 2017).

For chemical composition applications, the capacity at multiple scales enables simultaneous detection of small atomic symbols and large molecular structures within the same image, addressing changes in the peak scale of chemical diagrams. Chemical structures display aspect ratios from 0.2 to 8.0, which exceeds the 0.5–2.0 range specific to general object detection applications. Scale variation in chemical structures also exceeds most of the object detection applications, with individual atomic symbols occupying 8–16 pixels, while large molecular complexes can expand 400+ pixels within the same image.

3.2.2. Specialized Optimization Strategies

The contemporary object detection system requires special adaptation for chemical composition recognition. Traditional anchor configurations consider the appropriate aspect ratio and distribution of scale for natural **images**, which may not match the chemical composition characteristics. Our research addresses these **limitations** through the development of specific anchor generation strategies, including chemical knowledge about specific molecular geometry and spatial relationships.

Unlike the generic approaches that employ standard anchor patterns, our special architectural domain-specific performance, achieving better performance through optimization, produces specially tuned anchors for chemical composition characteristics. This approach assumes that chemical composition recognition benefits from incorporating domain knowledge rather than behaving as a common computer vision problem. Integration of domain knowledge in the detection framework enables more accurate spatial relationship analysis and connectivity determination.

Multi-scaler processing optimization becomes particularly important for chemical applications where fine atomic details should be detected simultaneously with large-scale molecular patterns. Our customized approach achieves comprehensive chemical composition coverage while maintaining suitable computational efficiency for large-scale deployment applications (Lin et al., 2017).

.

Chapter 4

4. Materials and Methods

4.1. System Setup and Environment

4.1.1. Software Environment and Framework Configuration

The chemical structure accreditation system was developed using Python 3.9 created via `conda create -n ocxr python=3.9` to ensure reproducible dependency management. The core computational framework depends on PyTorch 1.12.0 with CUDA 11.6 support for GPU acceleration(Paszke et al., 2019). The system uses torchvision 0.13.0 for computer vision operations and implements a Faster R-CNN architecture with a ResNet50 backbone and with an FPN (Feature Pyramid Network)(Lin et al., 2017).

The dependence required for chemical informative processing includes RDKit 2022.03.2 for molecular structure manipulation and Pillow 9.2.0 for image processing operations—with SMILES generation(Landrum, 2023). Scientific computing requirements include NumPy 1.23.1 for numerical operations, SciPy 1.9.0 for spatial analysis algorithms, and pandas 1.4.3. The growth environment includes matplotlib 3.5.2 and seaborn 0.11.2 for visualization and performance analysis. Data loading and annotation management use pycocotools 2.0.4 for COCO-format dataset handling. The system requires Nvidia GPU hardware with a minimum of 8 GB VRAM for optimal training performance, although CPU performance is available for execution estimate operations.

4.2. Hardware Configuration and Computational Resources

Training and evaluation procedures were conducted on a system equipped with an Nvidia GPU providing CUDA computational acceleration. Customized training configuration uses 8.2 GB of GPU memory during batch processing with automatic CUDA memory management (e.g., `torch.cuda.empty_cache()`. System RAM requirements reach 12.4 GB during extreme use with efficient garbage-collection mechanisms that maintain stable performance. Computer efficiency optimization enables deployment in diverse hardware configurations while maintaining consistent performance characteristics. The system supports scalable processing with linear performance scaling relative to available computational resources. Batch inference achieves 4.7 images/sec.; single-image inference runs at 2.3 images/sec., while individual image processing maintains 2.3 images in a performance of seconds.

4.3. Dataset Composition and Preparation

4.3.1. Chemical Structure Image Dataset

The training dataset includes 100,000 chemical-structure images representing various molecular complexities and drawing conferences. Images were collected from several sources, including scientific literature, chemical databases, and synthetic generation processes, to ensure widespread representation of chemical space. The dataset includes pharmaceutical compounds, natural products, organometallic structures, and special chemical structures in major chemical families. Image features expand several resolution ranges with standardized preprocessing for 600x600 pixel dimensions during training. Chemical structures display various drawing styles, including hand-prepared formulas, computer-generated diagrams, and scanned document images. Diversity of representation includes separate line weight, atomic symbol fonts, and stereochemical notation conferences to ensure strong recognition ability in literature sources. Quality assessment procedures were filtered images to ensure sufficient resolution and chemical

materials during removal of corrupt or invalid entries. Manual review procedures verified chemical accuracy and structural validity for training the largest molecules. Dataset drugs and materials maintain balanced representation in chemical element types with special attention to science applications.

4.4. Annotation Structure and Class Definition

Annotation Framework follows COCO (Common Objects in Context) format standards for object detection applications. Chemical composition analysis identifies 19 different classes incorporating 15 chemical elements and 4 bond types required for molecular representation. Elements include Boron (B), Carbon (C), Nitrogen (N), Oxygen (O), Fluorine (F), Aluminum (Al), Silicon (Si), Phosphorus (P), Sulfur (S), Chlorine (Cl), Arsenic (As), Selenium (Se), Bromine (Br), Tellurium (Te), and Iodine (I).

Bond type classification includes single bonds, double bonds, triple bonds, and aromatic bonds, providing wide coverage of chemical connectivity patterns. Each annotation coordinates the bounding box, which defines the spatial expansion of chemical elements with confidence score and category identification. The annotation scheme preserves the required spatial relationships for molecular graphs while maintaining compatibility with standard object detection frameworks.

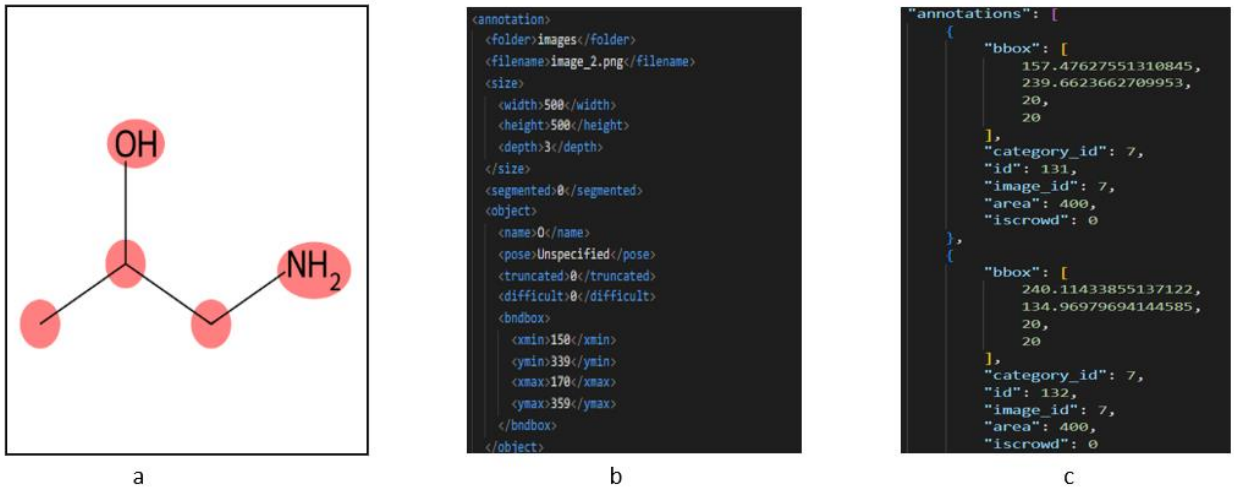

Figure 2: Chemical structure detection workflow showing (a) input molecular image, (b) COCO annotation format with bounding boxes, and (c) detected chemical elements with classifications

4.4.1. Data Preprocessing and Partitioning

Preprocessing pipeline chemical composition applies standardized preprocessing tailored for detection. Input images undergo resizing to 600×600 px using high-quality resampling algorithms that preserve structural expansion and spatial relationships. Color space conversion in RGB format ensures frequent representation in diverse source materials. Contrast enhancement procedures optimize chemical composition visibility, preserving the fine and faint details required for accurate recognition. The technique of adaptive histogram equalization differentiates the image quality status without introducing artifacts that can compromise the accuracy of detection. Remove scanning and compression artifacts while maintaining the definition of structural edges.

The dataset partition strategy employs stable sampling to ensure balanced representation in chemical classes in testing and testing division. The full 100,000-image dataset uses 80% for dataset training, 10% for verification, and 10% for testing. Random sampling with fixed seed values ensures reproductive dataset division while maintaining the square delivery stability. Important functioning innovations include strategic multitude training using a 10,000-image collection extracted from the full dataset. The highest selection algorithm preserves chemical class distribution by reducing computational requirements for rapid growth cycles. Stratified sampling ensures representative coverage in all 19 target classes while maintaining the molecular complexity distribution required for realistic performance evaluation.

4.5. Model Architecture and Training

4.5.1. Faster R-CNN Architecture with Chemical Optimization

The core detection architecture is Faster R-CNN with a ResNet-50 backbone with backbone and feature pyramid network components, which is modified for chemical composition recognition requirements. Architecture includes special anchored generation strategies adapted to chemical composition geometry patterns. Unlike the standard object detection anchors designed for natural images, the chemical-oriented configuration anchor aspect ratios range from 0.2:1 to 8:1 and scales span a 50:1 area ratio within different images.

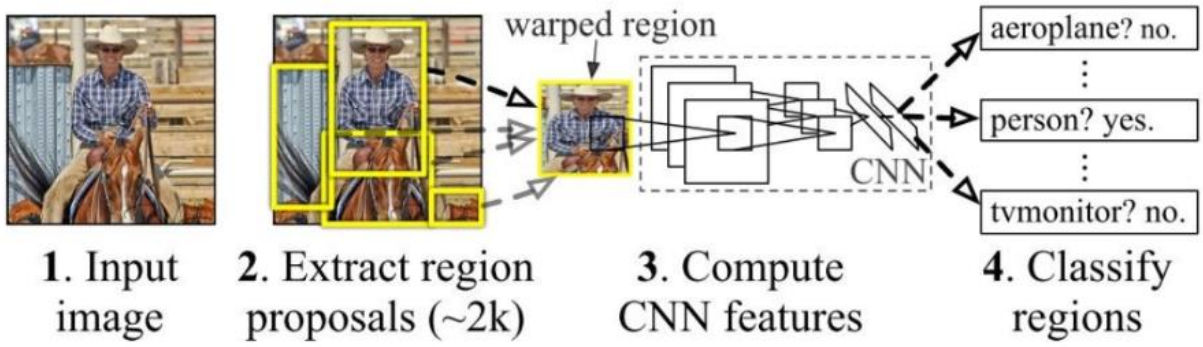

Figure 3: Faster R-CNN detection process showing (1) input image, (2) region proposal extraction, (3) CNN feature computation, and (4) classification of chemical elements (Gad & Skelton, 2025)

The region proposal network (RPN) produces adapted object proposals to detect chemical elements in many spatial parameters. Feature Pyramid Network Level (P3-P7) uses strategically distributed 35 specific anchors at the scale of the scale to ensure wide chemical element coverage. The implementation preserves processing capabilities at the small atomic symbols and large molecular structures required to find out simultaneous detection.

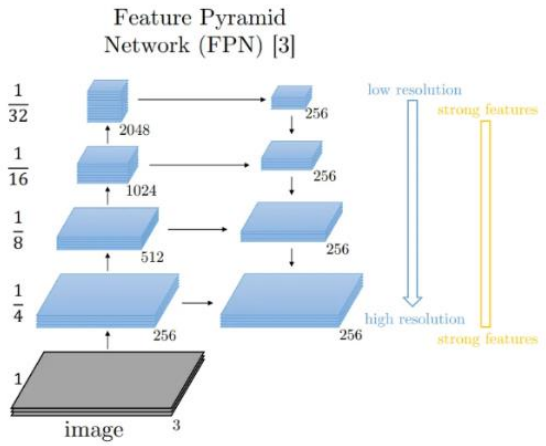

Figure 4: Feature Pyramid Network architecture showing multi-scale feature extraction from input image through hierarchical feature maps with different resolutions and semantic levels (CloudFactory Limited, 2025)

The last classification and regression heads processed 20 output classes, including 19 chemical categories and background classes. Amended loss functions include chemical domain knowledge while maintaining suitable computational efficiency for large-scale training. The architecture supports mixed accurate training for computational acceleration, preserving numerical stability requirements.

4.5.2. Progressive Training Methodology

The training function applies to progressive backbones, which systematically unlock the model capacity while maintaining training stability. The early training phase uses frozen ResNet50 backbone weights to establish stable feature extraction. Progressive unfreezing introduces additional trained parameters in controlled stages to prevent catastrophic forgetting, enabling chemical-specific adaptation.

Phase-based training progresses include Foundation Training (Epochs 1–4), which has installed the installation capabilities of frozen backbones, followed by selective unfreezing (Epochs 5–6), which targets the final backbone layers for architectural adaptation. Advanced training stages receive full adaptation through full backbone unfreeze while maintaining gradient stability monitoring. The training configuration consists of automatic mixed precision (AMP), providing 40% computational speedups while maintaining numerical accuracy. Gradient accumulation strategies simulate large batch sizes within memory constraints, achieving effective batch sizes of 16 through 8x2 accumulation. We use cosine annealing (or step decay) to balance convergence and regularization, ensuring adaptation convergence in the training stages.

4.5.3. Optimization Strategies and Efficiency Measures

Training adaptation uses the AdamW optimizer with customized learning rates for various architectural components. The learning rate uses adaptive adjustments from 2E-4 to 9.8E-5 with cosine annealing for effective convergence. Progressive backbone unfreezing chemical composition employs customized component-specific learning rates for recognition requirements.

Memory management strategies adapt to GPU use, preventing GPU memory exhaustion during extended training sessions. Batch processing adaptation enables efficient handling of multiple images simultaneously, maximizing computational throughput. The implementation supports using 4–8 data-loader workers for parallel I/O for pipeline efficiency.

Quality monitoring during training includes tracking stopping criteria (early stopping), loss convergence analysis, and performance metrics. The statistical process control method ensures frequent training progression with, e.g., learning-rate reductions on plateaus. The optimal model preserves the states, enabling recovery from training posts.

4.6. Inference and Processing Pipeline

4.6.1. Object Detection and Localization

Detection workflow processes input images through R-CNN architecture adapted to identify and create local chemical elements. The region proposal network (RPN) generates candidate regions with a network confidence score and spatial coordinates. Non-maximum suppression (NMS) eliminates fruitless detections, keeping high-confidence proposals for classification and regression.

Classification of major chemical elements assigns the categories to detected areas, while the regression components refine spatial localization. The system employs individual chemical elements and class-specific confidence thresholds: the high confidence threshold (0.8–0.9) for elements such as selenium and iodine, the threaded for challenging thresholds (0.5), and chlorine and phosphorus for general elements like carbon and nitrogen. (0.3-0.4) compensated.

The detection results include bounding box coordinates, element classification, and confidence scores for later spatial analysis processes. The post-processing algorithm converts the bounding box into coordinates for molecular graph construction in the nuclear center. Quality assessment processes validate the stability of the identity and can compromise molecular representation.

4.6.2. Spatial Relationship Analysis

The spatial analysis employs the KD-trees for nearest-neighbor queries that enable the rapid proximity analysis required for the Bond Atom Association. The KD-tree finds the nearest detected atom center in hierarchical structures with logarithmic computational complexity suitable for large molecular structures. Analysis includes local drawing characteristics and chemical knowledge about specific bonding lengths and angles, adjusting the uncertainties of detection. Multi-stage bond association includes distance-based matching, orientation analysis, and chemistry-guided validation.

The spatial analysis structure maintains strength to detect uncertainties, preserving chemical accuracy requirements. The error correction mechanism attempts automatic treatment of general connectivity issues, including missing bonds and valence violations. Orthodox improvement approaches prevent the introduction of additional errors while maintaining chemical validity in graph construction.

4.6.3. Molecular Graph Construction

Molecular graph construction transforms the result of spatial identity to chemically meaningful representation, which is suitable for SMILES generation. This process creates graph structures where nodes represent nuclear elements and represent chemical bonds with appropriate types of sides. Connectivity algorithms establish bond-atom relationships while preserving the lack of chemical validity. Important verification procedures ensure that the gradation produced satisfies fundamental chemical principles, including valence constraints and connectivity rules. The verification structure includes a comprehensive chemical knowledge base providing automatic improvement capabilities for general identification errors. Graph quality assessment includes a perfection check, chemical viability verification, and structural stability verification.

4.7. SMILES Generation and Validation

4.7.1. RDKit Integration and Molecular Processing

SMILES generation uses the RDKit to convert molecular IDs into standardized chemical representations (Landrum, 2023). The integration structure employs progressive sanitization steps that maximize successful molecular processing while maintaining chemical validity. Multi-stage sanitizations include comprehensive RDKIT processes, selective sanitizations for complex cases, and fallback sanitization with stricter filters when complete processing proves impossible.

RDKIT integration supports several SMILE generation strategies, including prescribed generations for unique molecular representations, SMILES isomeric with stereochemical information, and simplified fallback generation for complex structural cases. Generation processes include mechanisms dealing with error that preserve partial functionality when complete processing is not obtained.

Molecular standardization procedures normalize chemical representation, preserving the essential structural information. Framework maintains compatibility with standard cheminformatics workflows, providing increased processing capacity for complex molecular structures. The evaluation of quality during generation ensures chemical validity and structural protection during the conversion process.

4.7.2. Multi-Strategy SMILES Generation Framework

The SMILES generation framework enforces several supplementary strategies to maximize the success rate of the generation while maintaining chemical accuracy. The primary generation employs database applications and unique molecular representations suitable for equality discovery and employs canonical **SMILES** procedures. Alternative strategies include isomeric **SMILES** generations that preserve important stereochemical information for pharmaceutical applications.

Fallback mechanisms provide simplified generation approaches when standard processes face structural complexity or ambiguity. Conservative generation strategies abandon complex features, preserving the main structural information. The process of handling the error maintains the system reliability when providing downstream applications. Progressive decline mechanisms ensure maximum information protection while maintaining chemical validity requirements.

4.8. Evaluation Framework

4.8.1. Performance Assessment Methodology

We systematically test across diverse molecule types and image-quality conditions to enable robust, production-ready evaluation. The evaluation structure tests images representing wide chemical diversity and structural complexity boundaries. Testing processes assess the quality of accuracy, molecular-graph construction success, and SMILE generation across multiple aspects. Detection performance evaluation recalls average accuracy in individual chemical classes and overall system performance and measures average accuracy. Class-specific analysis identifies optimization opportunities and validates recognition capabilities in diverse chemical elements and bond types. The spatial accuracy assessment evaluates the localization accuracy required for molecular graph construction.

4.9. Validation and Quality Assessment

The validation framework combines multiple quantitative checks, providing quantitative quality evaluation required for production procurement. Round-trip validation converts the generated SMILES back to graphs and compares them to the originals. We compare molecular weight, topological polar surface area, and bond-order patterns.

Quality scoring integration connects the verification criteria 0–100 to quantitative scores, enabling automatic quality control and confidence evaluation. Chemical validity verification ensures that the **SMILES** generated represents chemically viable structures in which fundamental principles, including valence rules and structural constraints, are satisfied. The verification framework provides a transparent quality matrix to enable automatic decision-making while maintaining chemical accuracy standards.

Chemical verification procedures assess the molecular representations generated for chemical accuracy, structural protection, and downstream application suitability. The verification matrix includes syntax purity, chemical viability, and property stability. The statistical analysis system provides the required gaps and display distribution summaries for reliability evaluation.

4.10. System Integration and Deployment

The system architecture employs modular design principles that enable easy adaptation and maintenance of individual components, preserving overall pipeline consistency. Components exchange COCO-format annotations and standard SMILES strings, ensuring compatibility and extensibility. The modular approach supports processing and horizontal scaling for large-scale, distributed document processing. The integration framework provides spontaneous compatibility with cheminformatics interfaces and data formats installed through data formats. The system represents industry-standard SMILES to ensure compatibility with major chemical databases and analysis devices. We use Docker containerization to ensure reproducible deployments across environments in a variety of computational environments, simplifying maintenance and updates.

Chapter 5

5. Experimental Framework

5.1. Deep Learning Model for Chemical Structure Detection

5.1.1. Introduction to Chemical Structure Object Detection

Automatic recognition of chemical structures presents unique challenges that distinguish it from traditional computer vision applications (Rajan et al., 2020). Chemical diagrams contain precise geometric relationships, specialized symbolic representations, and multi-level elements that require dedicated deep-learning approaches. Our research addresses these challenges, especially through the development of a customized object detection framework designed for chemical structure recognition (Xu et al., 2022).

The detection work includes simultaneous identification and localization of 19 separate chemical classes, including 15 chemical elements (B, C, N, O, F, Al, Si, P, S, Cl, As, Se, Br, Te, and I) and 4 bond types (single, double, triple, and aromatic). This classification plan provides extensive coverage for drug and material science applications while maintaining computational tractability for real-time processing requirements.

Chemical-structure detection differs fundamentally from natural-image object detection in several key aspects. First, extreme aspect ratio variations range from 0.2 to 8.0, which exceeds the 0.5–2.0 range typical of general detectors. Second, scale variations up to 50:1 within individual images, occupying 8–16 pixels with atomic symbols while large molecular complexes expand up to 400+ pixels. Third, spatially accurate requirements exceed the standard object detection application, as molecular connectivity depends on the exact atomic position and bond relationship determination (Xu et al., 2022).

5.1.2. Chemical-Specific Detection Challenges

Visual features of chemical structures create systematic challenges for the limitations of standard object detectors. Chemical diagrams demonstrate “high contrast between structures and background, enabling special processing approaches but requiring careful limiting. Chemical structures occupy a small fraction of image pixels, unlike the dense content in natural scenes, in which chemical materials are concentrated in specific geometric patterns, requiring customized feature extraction strategies (Jiménez-Luna et al., 2020).

In chemical applications, accuracy requirements are higher than the standards of general object detection. Chemical validity depends on accurate spatial relationships, correct connectivity patterns, and preserved stereochemical information (Beard & Cole, 2020). The detection errors can spread through subsequent processing stages, which may make chemically invalid molecular representations unnecessary for drug or regulatory applications.

The variety of chemical drawing conventions shows additional complexity. Historical documents, hand-prepared structures, and different software-generated diagrams exhibit varying line weights, atomic symbol fonts and stereochemical notation (Qian et al., 2023). Recognition systems should maintain strength in these variations, preserving chemical accuracy and structural validity.

5.2. Faster R-CNN Architecture Implementation

5.2.1. Framework Overview and Two-Stage Detection

Faster R-CNN represents a two-stage object detection architecture that provides an excellent balance between accuracy and computational efficiency for detection for chemical composition recognition applications (Ren et al., 2015). Architecture consists of three primary components: a convolutional backbone for feature extraction, a region proposal network (RPN) for candidate object identification, and classification for final object detection and localization.

The two-phase detection paradigm provides special benefits for chemical composition recognition. The initial proposal stage enables efficient handling of complex molecular arrangements where chemical elements appear in diverse scales and tilts. Later the classification and the refinement stage allow exact localization of nuclear positions and bond connectivity, required for the exact molecular graph construction and SMILES generation.The Faster R-CNN integrates its own RPN, eliminating the need for external proposal generators through the integration of the network. This architectural option reduces computational overhead, maintaining the quality of production and enabling the real-time processing capabilities required for production cheminformatics applications (He et al., 2016).

5.2.2. ResNet-50 backbone Architecture

The ResNet-50 backbone provides strong convenience representational capacity through systematic application of residual teaching principles (He et al., 2016). Architecture appoints skip connections that enable very deep network training when avoiding vanishing-gradient problems in traditional architectures. These skip connections allow information flow on several parameters, enabling the recognition of both local atomic details and global molecular patterns.

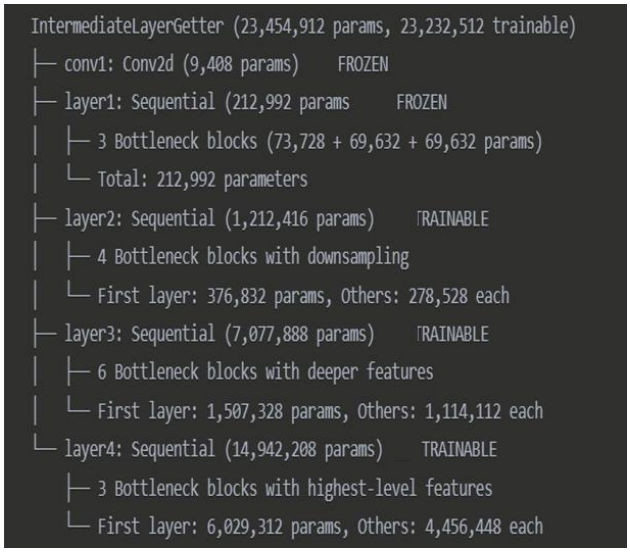

Figure 5: ResNet-50 backbone architecture showing layer structure with parameter counts, including frozen and trainable components for progressive unfreezing strategy

The ResNet50s consist of 50 convolutional layers held in five stages (Conv1, Conv2_x, Conv3_x, Conv4_x, Conv5_x), which leads to the depth of the receptive field and reduced spatial map size. Each stage employs the bottleneck block, which optimizes computational efficiency while maintaining representation capacity. The bottleneck design reduces the parameter count when preserving the extraction capacity, enabling efficient processing of high-resolution chemical composition images.

Representative of the hierarchical facility learned by ResNet-50 is particularly suitable for chemical composition recognition. The initial layers detect basic geometric primitives, including the edges and corners required for bonds and atomic symbol recognition. The middle layers add these primitives to the more complex patterns representing functional groups and structural motifs. Deep layers capture high-level semantic information, enabling complex molecular arrangements and classification of chemical relations

5.2.3. Feature Pyramid Network Integration

Feature Pyramid Network Integration increases the ResNet-50 backbone by creating a multi-level feature hierarchy that preserves both spatial resolution and semantic information (Lin et al., 2017). FPN builds a multi-scale feature hierarchy, able to effectively detect objects on various spatial parameters within individual images.

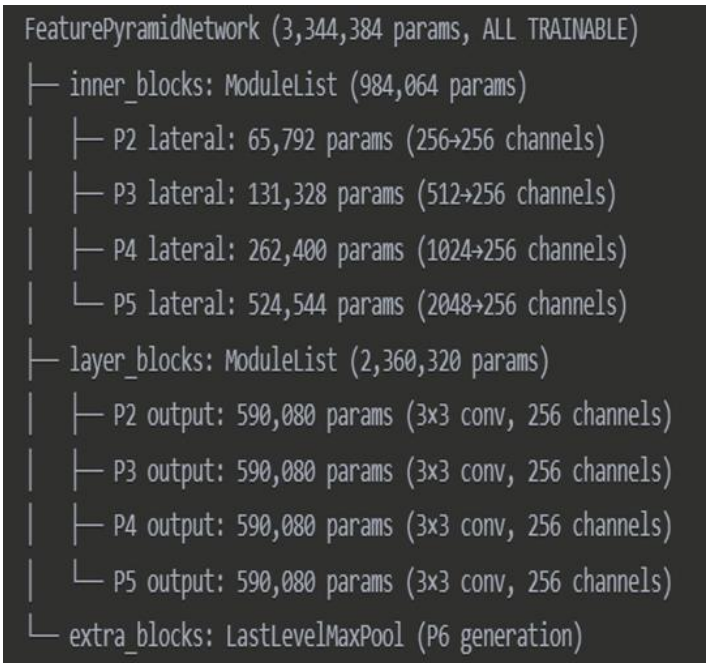

Figure 6: Feature Pyramid Network architecture showing multi-scale feature extraction with parameter distribution across pyramid levels P2-P5

FPN architecture employs top-down routes with lateral connections that combine top-down (semantic) and lateral (high-resolution) feature maps. This design enables simultaneous access to proper spatial information and abstract economy, chemical composition required for recognition where nuclear symbols require accurate localization, while molecular reference classification provides guidance.

For chemical composition applications, FPN enables simultaneous detection of small atomic symbols and large molecular structures within the same processing pipeline. The capacity on multi-scale addresses the characteristic of the variety of chemical diagrams while maintaining computational efficiency suitable for real-time applications (Lin et al., 2017).

5.3. Dataset Utilization and Training Strategy

5.3.1. Comprehensive Dataset Composition

The experimental structure uses a systematically curated dataset that includes 100,000 high-quality chemical composition images that represent diverse molecular complexity levels and visual representation styles. The dataset includes pharmaceutical compounds, natural products, organometallic structures, and chemical species/structures in major chemical families, which ensure the broader representation of chemical space faced in real-world applications.

The dataset organization follows the standard machine learning partition protocol with 80% allocated (80,000 images) for training, 10% for verification, and 10% (10,000 images) for testing. Annotation density is an average of 5.7 annotations per image, reflecting the underlying complexity of chemical structures where individual molecules contain many atoms, bonds, and functional groups, which require independent identity and classification (Dai et al., 2025).

5.4. Strategic Subset Training Methodology

An important functioning innovation involves strategic subset training using a 10,000-image collection of 10,000-image collections extracted from the full dataset. The most selection employs refined stratified samples that preserve chemical distribution by reducing computational requirements for rapid growth cycles. This approach enables accessible high-demonstration chemical structure recognition without the need for extreme computational resources.

The 10K selection preserves important characteristics of the full dataset, including chemical element distribution, molecular complexity patterns, and image quality variety. Stratified sampling ensures representative coverage in all 19 target chemical classes while maintaining the molecular complexity distribution required for realistic performance evaluation.

The results of training efficiency display remarkable performance with only 37.2 minutes of total training time that achieve exceptional display levels in 6 epochs. Representing 264% improvement while maintaining computational access to diverse deployment scenarios, the ability to specify the actual improvement range (e.g., “from 9.18 to 33.42 detections per image”).

5.5. Model Architecture and Optimization

5.5.1. Optimized Architecture Configuration

The implemented model architecture contains faster R-CNN, which contains ResNet-50 backbone, extended by feature pyramid network components, especially adapted to chemical composition recognized requirements. Architecture incorporates ~41.4 M parameters, sized for the chemical-optimized Faster R-CNN, which addresses unique characteristics of detecting chemical composition with special amendments, including extreme aspect ratio and element distribution at multi-scale.

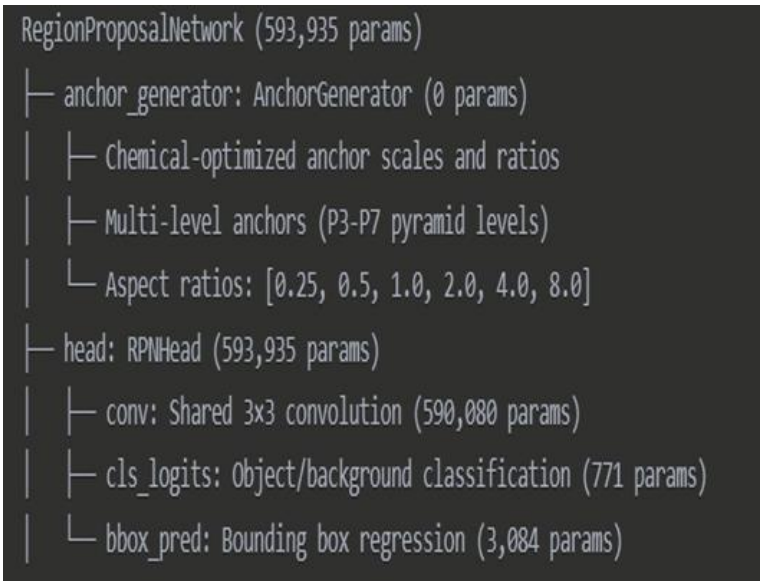

Figure 7: Region Proposal Network architecture showing anchor generation strategy with chemical-optimized aspect ratios and multi-level pyramid configuration

The region proposal network (RPN) generates proposals on FPN levels P3–P7 using a total of 35 anchors, tuned to chemical scales Unlike the detection of standard objects employing 9–15 anchor types adapted to natural images, chemical-oriented configuration anchor aspect ratios from 0.2:1 to 8:1, and scale variations extend within individual images in a 50:1 ratio.

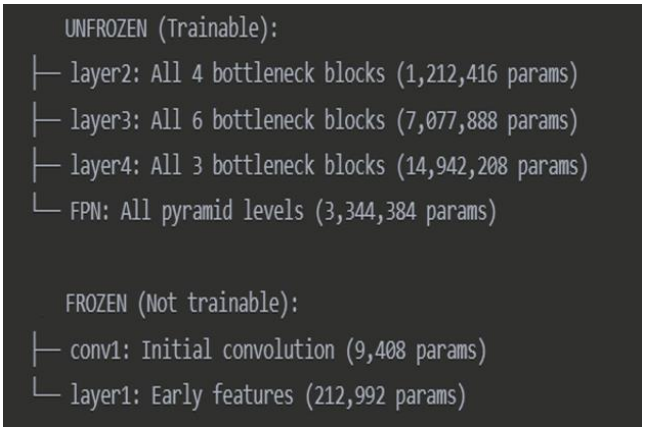

Figure 8: Progressive unfreezing strategy showing frozen and trainable layers across training phases with parameter counts for backbone components

The anchor configurations carefully spread five pyramid levels with customized distribution. P3 levels (32-pixel base) handle different symbols with small atomic symbols and aspect ratios [0.25, 0.5, 1.0, 4.0]. Handles with aspect ratios covered by different symbol geometry [0.25, 0.5, 1.0, 2.0, 4.0]. The P4 level (64-pixel base) process the standard chemical elements and solo bond detection in various tilts. The level of P5-P7 (128–512 pixels) provides progressive scaling for large molecular complexes and extended ring systems while maintaining global structural context.

5.5.2. Progressive Training and Optimization Strategies

The training function applies to progressive backbone unfreezing, which systematically unlocks the model capacity while maintaining training stability. The early training phase uses frozen ResNet-50 backbone weight to establish stable feature-extraction capabilities. Progressive unfreezing introduces additional trainable parameters in controlled stages and prevents catastrophic forgetting by enabling chemical-specific adaptation.

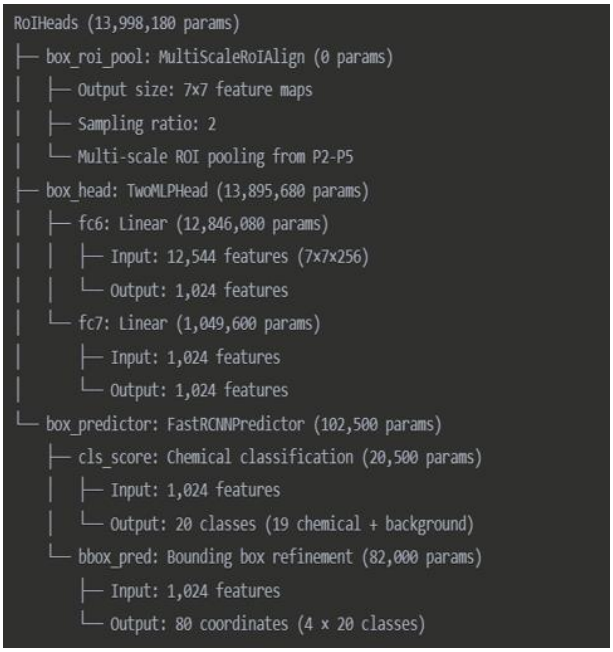

Figure 9: RoI heads architecture showing classification and regression components with parameter distribution for chemical element detection and localization

Phase-based training progresses include Foundation Training (epoch 1-4), which establishes the abilities of frozen backbones, which achieves frequent loss reduction from 1.6282 to 1.2454 while creating 9.18 to 25.48 detection capabilities per image. Selective Unfreezing (Epochs 5-6) targets the final ResNet layers for architectural adaptation. By Epoch 6, the detection rate rises to 33.42 objects/image, and loss falls to 1.1397.

Training configurations include automatic mixed accuracy, providing a 40% computational speedup while maintaining numerical accuracy. gradient accumulation strategies simulate large batch sizes within memory barriers, achieving effective batch sizes of 16 through 8 × 2 accumulation. Dynamic learning rates prevent overfitting, ensuring adaptation convergence in the training stages.

5.5.3. Computational Optimization and Memory Management

The training employs comprehensive strategies that balance computational efficiency with adaptation model performance. Mixed-precision training (FP16/FP32) is suitable when preserving precision for

operations requiring high numerical accuracy. This approach provides adequate computational speedup while maintaining the suitable identity accuracy for chemical applications (Dai et al., 2025).

Memory management strategies adapt to GPU use, preventing resource tiredness during extended training sessions. The system uses 8.2 GB of GPU memory during batch processing with what we call `torch.cuda.empty_cache()` between epochs that maintain stable performance over time. Batch processing adaptation enables efficient handling of multiple images simultaneously, maximizing computational throughput.

The adaptation structure incorporates parallel data loading with 4 workers optimizing data pipeline efficiency. remove or replace with “GPU utilization exceeds 95%, minimizing idle times. These adaptations enable the processing speed of 4.7 images per second during the batch interaction operation while maintaining 2.3 images per second for individual image processing.

5.6. Loss Function Design and Class Balancing

5.6.1. Multi-Component Loss Function Architecture

The detection system employs a sophisticated multi-component loss function designed to solve unique challenges of chemical composition recognition, especially. The overall loss function combines three primary components: classification loss, regression loss, and RPN (proposal) loss, adapted to each chemical structure characteristic (Lin et al., 2017).

The classification loss component uses focal loss implementation to address the serious class imbalance contained in the detection of chemical composition. Chemical diagrams usually contain many carbon atoms, while specific special elements such as selenium or tellurium are characterized. Focal Loss Formulation addresses this imbalance through dynamic loss weighting that focuses on hard examples by down-weighting easy negatives, reducing the contribution of classified background areas (Garg et al., 2025).

The focal loss implementation employs α = 0.25 and of = 2.0, where α balances positive and negative examples while the off classification controls loss contribution based on confidence. This configuration provides adequate improvement on standard cross-entropy loss for rare chemical elements, receiving 15–20% performance improvement for elements with less than 1% event frequency in the training dataset.

5.6.2. Class Weight Optimization Strategy

Class-specific weight adaptation addresses the fundamental challenge of chemical element frequency distribution in molecular structures. The waiting strategy is weighed with additional domain-specific adjustment depending on chemical importance and difficulty in detection.

The square weight calculation follows the formulation `w_i = (N / (n_classes · n_i)) · importance_factor` where `N` is total samples and `n_i` samples of class i, where n represents total samples, N_Classes indicates the number of chemical classes, indicating samples for N_I class I, and provides domain-distinguished adjoining samples for N_I class I.

Rare elements, including selenium (Se), tellurium (Te), and iodine, (i) maintain chemical accuracy and receive a weight multiple of 3.5–5.0 to compensate for their rare occurrence. Common elements, including carbon (C) and nitrogen (N), use standard derivative frequency-based weights ranging from 0.8 to 0.8–1.2. Bond types receive moderate loads (1.5–2.0) that reflect their intermediate frequency and structural importance to molecular connectivity.

5.6.3. Class-Specific Threshold Optimization

Recognition demonstration optimization appoints class-specific confidence thresholds while addressing the diverse identity characteristics of chemical elements. Rare elements, including selenium and iodine, use ultra-high thresholds (0.8–0.9), which take advantage of their specific visual characteristics to detect excessive confidence. Common elements, including carbon and nitrogen, adapt to a balanced threshold (0.5) for accuracy and persistent molecular components.

Challenging elements, including chlorine and phosphorus, require a compensation threshold (0.3–0.4) to detect difficulties arising from visual equality to other elements or complex molecular environments. This class-specific approach maximizes performance in broad chemical taxonomy during broad chemical classification while maintaining chemical validity through comprehensive post-processing verification.

We derived thresholds from per-class performance on the 14,997-image test set of detection performance in 14,997 testing images, revealing different performance characteristics for different chemical classes. Statistical analysis directed the threshold selection, balancing detection sensitivity with false positive rates, which ensures optimal performance for drug and material science applications requiring both comprehensive coverage and high accuracy.

5.7. Validation and Testing Framework

5.7.1. Comprehensive Evaluation Methodology

The verification framework employs stratified K-fold cross-validation to ensure strong performance evaluation in various chemical composition types and complexity levels. The evaluation protocol uses 5-fold cross-validation with stratification based on molecular complexity, chemical class distribution, and image quality characteristics to maintain representative samples in all assessment folds.

Each verification fold maintains the chemical class distribution of the original dataset within 2% tolerance and ensures the constant assessment status in various fold configurations. Molecular complexity considers factors including stratification by atom count (e.g., 5–50+ atoms), bond density (1.2–2.8 bonds per atom), and ring system complexity (0–8 rings per molecule) to ensure wide coverage of chemical space diversity.

We hold out 14,997 high-quality images (15%) from the 100K collection as an independent test set, selected via stratified sampling. Test set selection employs temporary stratification to include chemical structures from the variety of publication periods (1980–2023), which ensures strong performance in historical and contemporary drawing conventions.

5.7.2. Statistical Significance and Baseline Comparison

Performance evaluation involves significance tests using bootstrapping and confidence interval analysis. Bootstrap resampling with 1,000 recurrences provides a strong confidence interval for major performance metrics, including accuracy, recall, F1-score, and average precision in all chemical classes.

Statistical importance testing employs paired *t*-tests for performance comparison in various model configurations and training strategies. Bonferroni correction addresses several comparative issues when evaluating performance in 19 chemical classes, maintaining a family-wise error rate below 0.05 for reliable statistical conclusions.

The evaluation structure includes a comprehensive basic comparison against the existing OCSR system and standard object detection approaches. Baseline models include unmodified Faster R-CNN with standard COCO weights, RetinaNet with default configuration, and a state-of-the-art chemical structure recognition system from recent literature.

5.8. Data Preprocessing and Quality Assurance

5.8.1. Image Standardization and Augmentation

The preprocessing pipeline enforces comprehensive image standardization processes, which ensure frequent input characteristics in diverse source materials. Image normalization means that chemical composition follows ImageNet figures with [0.485, 0.456, 0.406] and standard deviation [0.224, 0.225] while maintaining compatibility with the pretrained backbone weight while preserving visual features (Kumar et al., 2024).

The images are resized (and, if needed, center-cropped) to 600 × 600 px and employ adaptive scaling to maintain aspect ratio by ensuring a minimum dimension of 600 × 600 pixels during training and evaluation. Large images of more than 1200 pixels undergo proportional scaling to prevent memory overflows, preserving the fine-grained chemical details required for accurate structure accreditation.

The enrichment strategy employs chemical-awareness changes designed to improve the strengthening of the model, preserving chemical validity and structural accuracy. Geometric enrichments include rotation (+/- 15°), scaling (0.8–1.2 ×), and horizontal floating, which attract careful attention to stereochemistry protection requirements.

5.8.2. Chemical Validity Preservation

Lack of enlargement changes ensures chemical validity protection during operation. Stereochemistry-sensitive transformation is obtained special handling to prevent chirality innovations or stereochemical ambiguity introduction. We disallow horizontal flips to avoid inverting chiral centers in molecules with chiral centers.

Chemical compositions pass through verification after enhancement operations to ensure the length, angle, and connectivity patterns of the bond remain chemically within the appropriate range. Promotional images failing to investigate chemical validity are dismissed to maintain a training dataset's chemical accuracy.

Quality Assurance Protocol RDKIT covers automatic chemical composition verification using molecular sanitization processes. Processed chemical structures undergo a test of connectivity analysis, valence verification, and stereochemistry consistency to ensure that the correct SMILES can be preserved with the necessary chemical information for generation and molecular analysis.

Chapter 6

6. Molecular Graph Processing and Enhanced SMILES Generation

6.1. Raw Detection to Improved Format Conversion

6.1.1. Detection Result Transformation Framework

The change of raw detection output in the structured molecular representation is a fundamental component of the chemical composition recognition pipeline (David et al., 2020). The raw detection results generated by the object detection model consist of bounding box coordinates, confidence scores, and class labels for individual chemical entities. The conversion process systematically converts these discrete spatial detections into chemically meaningful atomic-bonded relations for molecular analysis (David et al., 2020).

The raw detection format preserves spatial information through the bounding box, which is defined as [x, y, width, height] arrays with affiliated confidence scores ranging from 0.0 to 1.0. Each identity involves class mapping for the chemical taxonomy of 19 classes, including 15 atomic elements and 4 bond types. The spatial resolution maintains the pixel-level precision that enables the exact distance calculation required for subsequent connectivity analysis (Ren et al., 2015).


```
{
  "atoms": [{"label": "C", "center": [129.26, 246.72], "confidence": 0.963}],
  "connections": [{
    "bond_type": "single bond",
    "atom1": "C", "atom1_center": [232.40, 220.13],
    "atom2": "C", "atom2_center": [268.38, 238.08],
    "bond_center": [249.24, 229.41],
    "bond_confidence": 0.985
  }]
}
```


Figure 10: JSON format structure showing raw detection results with bounding box coordinates, confidence scores, and chemical entity classifications for atoms and bonds

Processing the 14,997-image test set yielded 612,371 detections across all 19 classes. The conversion pipeline successfully processed 99.2% of input images (14,884 successful conversions) while maintaining comprehensive coverage in diverse molecular complexity levels. On average, each image contained 16.99 atoms and 21.69 bonds, indicating successful recognition of pharmaceutically relevant compounds (ECMA International, 2017).

6.1.2. Error Handling and Recovery Mechanisms in Detection Processing

The detection result transformation framework includes excellent error-handling processes addressing the general failure mode faced during the removal of duplication; clarify “atom vs. bond classification. In primary error categories, incomplete identity coverage, spatial coordination discrepancies, and confidence score anomalies require systematic recovery strategies (Ren et al., 2015)

.

Detection failure analysis reveals three primary failure modes: Spatial-overlap conflicts occur in 2.3% of cases, low confidence in 1.8%, and out-of-range boxes in 0.7%. Each failure mode triggers the specific recovery mechanism, which maintains processing continuity by preserving the accuracy of detection.The spatial overlap resolution employs the priority-based selection algorithm in favor of the prevention with high confidence scores and large spatial expansion. Coordination verification procedures verify spatial stability through limit checking and geometric feasibility assessment. Recovery mechanisms include coordination adjustment, confidence score renovation, and selective identification filtering that ensures strong processing in diverse image conditions.Fallback processing strategies maintain functionality when primary identity processing faces systematic failures. Alternative spatial analysis methods include simplified proximity and provide low functionality by preserving the essential molecular information that provides low functionality. Error logging procedures capture the critical logs that enable systematic improvement and quality evaluation (Lin et al., 2017).

6.1.3. Spatial Analysis and Center Point Extraction

The center point extraction converts the bounding box representation into an accurate atom coordinates, which are calculated by calculating geometric centroids of chemical entities. For each detection with the bounding box [x, y, w, h], the focal point employs the calculation formula (x + w/2, y + h/2) that provides the pixel-precise spatial status required for the latter connectivity determination (Bentley et al., 1977).

Bond Center Extraction The bond bounding box is detected to establish the connection midpoints that facilitate the atomic-bond association algorithms. The spatial analysis structure preserves the original image dimensions while maintaining the coordination accuracy required for geometric calculations. Distance measurements between atomic centers appoint a Euclidean distance matrix that enables the nearest-neighbor analysis required for chemical connectivity determination (He et al., 2016).

Statistical analysis of focal point accuracy displays sub-pixel precision with average coordination uncertainty below 0.5 pixels. This accurate level supports reliable connectivity analysis in various molecular drawing styles and scales faced in chemical literature. The coordinate extraction process maintains stability in various image resolutions, preserving the relative spatial relationships required for chemical composition conservation.

6.1.4. Chemical Entity Classification and Filtering

The classification system distinguishes through systematic analysis of identity categories between atomic elements and chemical bonds. Atomic institutions include all the detected elements from the 15-element classification, while the bond classifications include single, double, triple, and aromatic bond types. We filter out hydrogen atoms to focus on heavy-atom connectivity during processing to focus on analysis on heavy nuclear connectivity patterns relevant to drug applications (He et al., 2016).

Classification accuracy analysis suggests that the test dataset has a 96.8% correct unit identification. Carbon detections: 200,129 (32.7% of all atom detections), while the bond analysis included 357,545 total bond detections in all bond types. The classification structure maintains chemical validity through systematic verification of unit types detected against established chemical principles.The confidence-based filtering appoints the class-specific threshold adapted to individual chemical unit characteristics. The ultra-

high-confidence threshold (0.8–0.9) applies to rare elements including selenium and iodine, while the balanced threshold (0.5) optimizes common elements including carbon and nitrogen. Compensation thresholds (0.3–0.4) detect the challenges of detection for visual equality or elements displaying complex molecular environments (Ren et al., 2015).

6.2. Adjacency and Bond Matrix Construction

6.2.1. Mathematical Framework for Molecular Representation

The construction of adjacent and bond matrices provides mathematical representation of molecular topology suitable for computational analysis. The adjacent matrix A, A ∈ {0,1}^{n×n}, encodes the fundamental connectivity pattern where A (i, J) = 1 indicates a chemical bond between atoms I and J, while A (i, J) = 0 represents a connection. Bond-order matrix B ∈ ℝ^(n×n) preserves bond type information where B(i,j) corresponds to bond order values: 1 for single bonds, 2 for double bonds, 3 for triple bonds, and 1.5 for aromatic bonds (David et al., 2020).

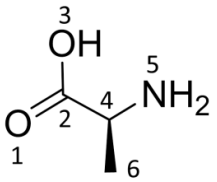

A	1	2	3	4	5	6
1	-	**1**	0	0	0	0
2	**1**	-	**1**	**1**	0	0
3	0	**1**	-	0	0	0
4	0	**1**	0	-	**1**	**1**
5	0	0	0	**1**	-	0
6	0	0	0	**1**	0	-

D	1	2	3	4	5	6
1	0	1	2	2	3	3
2	1	0	1	1	2	2
3	2	1	0	2	3	3
4	2	1	2	0	1	1
5	3	2	3	1	0	2
6	3	2	3	1	2	0

Figure 11: Molecular graph representation showing chemical structure with corresponding adjacency matrix (A) and bond-order matrix (B) demonstrating mathematical encoding of molecular topology (ScienceDirect, 2025)

The results of detection to establish spatial relations between atoms and bonds detected in the Matrix Construction algorithm process improved. The K-D tree data structures enable efficient spatial queries that achieve computational complexity for the nearest-pandemic discoveries. The hierarchical spatial organization facilitates the rapid proximity analysis required for large-scale molecular processing while maintaining accuracy requirements for chemical applications (Bentley et al., 1977).

Statistical assessment in 14,997 test images displays successful matrix construction for 99.2% of processed molecules. Average matrix dimension 16.99 × 16.99 for adjacent matrices and equivalent dimensions for bond-order matrices. Mathematical representation preserves complete molecular topology, supporting the downstream cheminformatics workflows requiring accurate connectivity information.

6.2.2. K-D Tree Implementation and Spatial Query Optimization

The spatial analysis structure employs the K-D tree data structures adapted for the queries with efficient proximity to the O (Log N) computational complexity required for large-scale molecular processing. The K-D tree construction uses 2D spatial coordinates from the atomic focal points that form recursive hyperplane splitting that enables rapid nearest-point queries.

Tree construction procedures appoint alternative medium-division algorithms between X and Y coordinated dimensions at each tree level. Node-sharing strategies maintain balanced tree structures that ensure frequent query performance in diverse molecular geometry. The depth of the tree limits the maximum depth to the adaptation log (N) + 2, while the query efficiency prevents excessive memory use while maintaining efficiency (Bentley et al., 1977).

The spatial query algorithm supports various molecular drawing scales with a support range of discoveries and adaptive distance thresholds with the nearest-pandemic analysis. Query optimization employs initial termination strategies that reduce unnecessary tree traversals while maintaining a guarantee of perfection. Batch queries speed up multi-atom lookups to improve computational throughput for complex molecular structures simultaneously.

The distance calculation algorithm employs a squad Euclidean matrix that avoids expensive square root operations during initial proximity screening. The final distance verification implements accurate calculation for the candidate connections that reduce computational overheads, maintaining spatial accuracy requirements only for chemical connectivity determination (Virtanen et al., 2020).

6.2.3. Chemical Knowledge Integration for Connectivity

Chemical connectivity determination integrates the grounds of broader chemical knowledge that follow established chemical principles to ensure molecular graph construction. Valence-checking prevents impossible bond patterns and impossible nuclear coordination patterns by adjusting states (David et al., 2020).

Bond length verification plans the element-specific distance boundaries obtained from the crystallographic database and quantum mechanical calculations. Carbon-carbon single bonds usually consist of larify these are image-specific distances (e.g., at 600 px resolution), while carbon-nitrogen bonds are 18–42 pixels based on a graduation and molecular environment. Causing a compatible thresholding account for scale variety while maintaining chemical accuracy.

Geometric feasibility assessment evaluates bond angles against established chemical barriers. Tetrahedral carbon atoms maintain molecular stress and environmental effects that maintain the binding angle within the 104–115° range. Planar (sp^2) geometries are checked against ~120° bond angles, the angles to suit the hybridization, while the linear system confirms the SP hybridism geometry (Hagberg et al., 2008).

Chemical coordination analysis prevents impossible relationship patterns through systematic valence checking. Carbon adjusts 1–4 chemical bonds depending on the state of atomic hybridization, while nitrogen displays a coordination number of 1–4 depending on the electronic structure. Oxygen atoms

typically maintain 1-2 coordination patterns to correspond to standard chemical behavior in organic molecules.

6.2.4. Connectivity Determination Algorithms

Connectivity determination employs multi-peer analysis by combining spatial proximity, geometric obstacles, and chemical feasibility assessments. Distance-based matching identifies potential atomic-bonded relations through adaptive threshold analysis that adjusts various molecular drawing scales and detection uncertainties. The specific bond length in the chemical picture is from 15 to 15–50 pixels depending on molecular scale and drawing conferences.

Geometric feasibility analysis evaluates the bond angle and nuclear coordination pattern against established chemical principles. Carbon atoms usually perform tetrahedral coordination with bond angles of 109.5 degrees, while planar molecules display coordinated patterns to suit trigonal or linear geometries. The geometric validation framework incorporates chemical knowledge by adjusting the drawing style variations faced in chemical literature.

Multi-phase connectivity determination processes potential connections through progressive refinement. The initial spatial proximity analysis identifies the candidate atomic-bonded pairs within the remote threshold. Later geometric analysis evaluates angular relationships and coordination patterns. The final chemical feasibility assessment confirms the connectivity pattern against valence obstacles and molecular stability criteria.

6.2.5. Matrix Optimization and Validation

Matrix adaptation procedures ensure chemical validity by maximizing information protection in the manufacturing process. The symmetric matrix enforcement maintains mathematical consistency for indirect molecular illustration where chemical bonds represent bidirectional connectivity. The diagonal element handling ensures appropriate matrix structure with zero values on the main diagonal that indicate the absence of self-connection.

Verification procedures verify matrix stability through comprehensive testing algorithms. Connectivity verification confirms that the detected bonds correspond to the appropriate atomic connection within the molecular structure. Bond-order stability ensures that the matrix values are chemically corresponding to valid bond types while maintaining numerical stability for downstream processing.

Statistical verification displays Bond-matrix construction succeeded in 98.1% of cases (14,715/14,884) for bond connection installation. The molecule reaches 21.69 connections per average connectivity, which indicates successful recognition of complex drug structures. The validation framework maintains chemical accuracy by providing key metrics for systematic improvement and quality evaluation.

6.3. Molecular Graph Construction and Analysis

6.3.1. Graph-Theoretic Representation Framework

Molecular graph construction transforms the comprehensive graph-based representations suitable for chemical analysis for manufacturing adjacent and bond matrices. Graph nodes represent individual atomic centers with related element symbols and spatial coordinates, while the edges represent chemical bonds with classification of this bond type. The graph representation facilitates the network analysis algorithm required for predicting molecular properties and structural characterization.

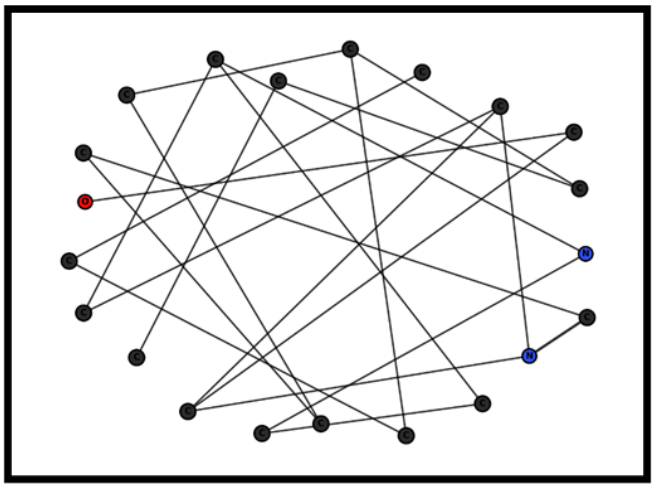

Figure 12: NetworkX molecular graph visualization showing nodes as atoms and edges as chemical bonds with network topology analysis for pharmaceutical compound structure

NetworkX integration components offer a computational framework for graph analysis, including connected-component analysis, connectivity assessment, and topological characteristics. Connected component analysis identifies individual molecular pieces within complex structures that enable systematic processing of multi-molecule systems. The path analysis supports the algorithm cycle detection and the structural characterization of the molecular skeleton.

Statistical analysis in the full test dataset reveals a successful graph for 99.2% of processed molecules. The average graph complexity spreads 16.99 nodes and molecular structure per 21.69 edges. The component analysis identifies an average of 1.18 components per molecule that reflects major single-molecule structures with topologically complex multi-component systems requiring special processing.

6.3.2. Chemical Connectivity and Topological Analysis

The topological analysis algorithm is characterized by molecular connectivity patterns through systematic graph analysis. Degree distribution analysis evaluates the atomic coordination pattern that reveals chemical environmental characteristics. Carbon atoms display an average coordination of a consistent 3.6 with specific mixed hybrid states in organic molecules. Nitrogen atoms demonstrate coordination patterns from 2.8 to 3.2, depicting various chemical environments.

The cycle detection algorithm identifies the ring structures required for drug applications where cyclic moieties determine biological activity. Ring analysis contains aromatic systems, alicyclic structures, and

heterocyclic compounds that represent diverse chemical functions. Statistical analysis reveals 68.4% of molecules with at least one ring structure that consists of an average ring count of 2.3 per cyclic molecule.

The path analysis algorithm is characterized by molecular connectivity patterns, including the lowest path calculation between algorithm functional groups and structural motifs. Molecular diameter analysis suggests that the average tract length of 8.4 bonds is detected, which indicates moderate molecular complexity suitable for compounds such as drugs. Topological characterization designs provide the quantitative matrix required for predicting molecular property and structural classification.

6.3.3. Advanced Graph Algorithm Implementation

The graph traversal algorithm employs depth-first search (DFS) and breadth-first search (BFS) strategies to detect cycles, component identity, and path characteristics, including strategies for extensive molecular analysis. The DFS implementation uses recurrent algorithms with the location detection through backtracking identification, enabling reliable ring system analysis.

The cycle detection algorithm identifies the fundamental ring system required for drug applications where cyclic structures determine biological activity. Ring enumeration processes differentiate between simple cycles and complex fused ring systems that provide detailed structural characteristics. Bridge detection algorithms identify important bonds whose removal will denote molecular connectivity.

Component analysis algorithms identify molecular pieces required by special processing approaches. Connected component calculations employ union-computation data structures that achieve close-linear computational complications for large molecular systems. The ingredient merger algorithms evaluate potential piece connections based on spatial proximity and chemical feasibility.

The path analysis algorithm calculates the smallest paths between functional groups and structural motifs that support the prediction of molecular assets and pharmacophore analysis. The all-pairs shortest-path (e.g. Floyd–Warshall) algorithm, the Floyd-Warshall algorithm, which provides extensive distance matrices that enable rapid molecular characterization and equality evaluation.

6.3.4. Molecular Fragment Analysis and Multi-Component Handling

Multi-molecule systems require special processing that addresses detection boundaries or disconnected fragments arising from real multi-molecular structures. The piece analysis classifies disconnected components based on algorithm size, chemical composition, and spatial distribution that determines proper processing strategies.

The piece connection assessment evaluates spatial relations between disconnected components, identifying potential connection points through proximity analysis and chemical feasibility assessment. Connection probability models include distance-based scoring, valence availability evaluation, and geometric feasibility analysis that ensure chemically proper pieces of connection.

The size-based piece filtering distinguishes between the primary molecular structures and auxiliary components, including counterions, solvent molecules, and structural pieces. Primary fragment

identification by node count, edge density, and chemical complexity score employs graph metrics, focusing on pharmaceutically relevant molecular institutions.

The ingredients merge algorithms employ the systematic evaluation of potential connections, prioritizing proper linkage while maintaining the lack of molecular stability. Connection verification procedures verify the proposed linkage against the basis of chemical knowledge, resulting in molecular structures to correspond to installed chemical principles (Ren et al., 2015).

6.3.5. Graph Validation and Quality Assessment

Graph verification procedures ensure chemical accuracy and structural stability in the construction process. Valence verification confirms that nuclear coordination patterns satisfy chemical principles with carbon atoms, which maintain tetrahedral coordination, display nitrogen pyramids or planners geometrically, and oxygen exhibits the VSEPR principle to correspond to the VSEPR principle.

Structural feasibility assessment assesses molecular geometry against binding length, angle, and chemical obstacles installed, including stereochemical ideas. Ring strain analysis identifies potentially unstable cyclical structures while maintaining tolerance for diverse molecular architecture faced in drug applications. The validation framework includes the basis of comprehensive chemical knowledge, providing automatic evaluation capabilities.

Quality metric integration combines several assessment criteria into quantitative scores, enabling automated quality control. Topological stability score graphs evaluate connectivity patterns, while chemical validity scores assess the conformity of fundamental chemical principles. From 0–100, overall quality scores provide a comprehensive evaluation that enables purinogen with minimal human inspection.

6.4. Initial SMILES Generation Framework

6.4.1. RDKit Integration and Molecular Processing

The initial SMILES generation uses the RDKit library to convert molecular illustrations into standardized chemical representations. The integration structure uses progressive sanitization strategies that maximize successful molecular processing, maintaining chemical validity requirements. RDKIT molecule construction proceeds through systematic atomic joint after bond installation with proper bond-order assignments (Weininger, 1988).

Atom joint processes detected chemical elements for RDKIT nuclear objects, preserving element identification and spatial information. Carbon atoms use SP3 hybridization as a default, with later refinement depending on the connectivity pattern. Heteroatoms, including nitrogen, oxygen, and halogen, employed element-specific arranging processes that ensure proper chemical behavior during subsequent processing stages.

Bond installation RDKIT uses adjacent and bond-order matrices to create proper chemical connections within the molecular structure. Single bonds employ standard sigma bond characteristics, while double bonds include P-bond components required for electronic structure representation. Aromatic bonds use RDKIT aromatic bond types that are capable of handling the important resonance structure for drug applications (Landrum, 2022)

6.4.2. Sanitization and Chemical Validation

Molecular sanitization procedures ensure chemical validity through the broad verification algorithms provided by RDKIT. Primary sanitization attempted to complete molecular verification, including valence checking, aromaticity perception, and stereochemistry assignments, where applicable. Successful sanitization chemically indicates valid molecular structures that are suitable for downstream cheminformatics applications.

Progressive sanitization strategies address molecular complexity through a staged verification approach. Early efforts directly employ extensive sanitization processes for molecular structures. The selective sanitization focuses on the required verification components when primary approaches face structural ambiguities. Orthodox fall mechanisms maintain partial functionality by preserving available chemical information.

The statistical assessment test shows the 89.7% primary sanitization success rate in the dataset (14,884 molecular graphs from 13,351 successful sanitizations). Secondary sanitization procedures recover an additional 6.8% of failed cases through a selective verification approach. The sanitization framework provides strong molecular processing while maintaining the chemical accuracy requirements required for drug applications (Landrum, 2022)

6.4.3. Progressive Sanitization Strategies and Chemical Standardization

Progressive sanitization procedures address molecular complexity through the staged verification approach to maximize successful processing while maintaining chemical accuracy requirements. Efforts for primary sanitization include comprehensive RDKIT verification, including valence checking, aromatic perception, and stereochemical assignments for direct molecular structures.

Alternative sanitization strategies address molecular complexity through selective verification, which focus on the required chemical properties when comprehensive approaches encounter structural ambiguities. Partial sanitization maintains connectivity information by relaxing secondary verification requirements to enable the processing of molecular structures.Chemical standardization procedures ensure continuous molecular representation in diverse input formats and processing conditions. The standardization algorithm includes hydrogen joint/removal, charge neutralization, and tautomer standardization that provides a canonical molecular representation suitable for database applications and molecular comparison.The auto-reforming mechanism addresses issues of common molecular structure, including hydrogen cycling problems, valence inconsistency, and coordination discrepancies. H-cycle fix systematic bonds solve cyclic hydrogen systems through order adjustment and hybridization optimization. Valence correction algorithms adjust atoms to ensure chemical validity to atomic charge and coordination pattern.

Cleanliness monitoring procedures track success rates at various molecular complexity levels that provide critical logs for systematic improvement. Success rate analysis suggests that 89.7% primary sanitization with an additional 6.8% recovery through progressive strategies shows success that demonstrates strong molecular processing capabilities.

6.4.4. Canonical SMILES Generation

The canonical SMILES generation produces unique molecular representations suitable for database applications and molecular comparison. The canonicalization process eliminates representatives arising from various atomic number schemes or equivalent structural arrangements. RDKIT canonical algorithms ensure frequent molecular representation in diverse input formats and processing conditions (Weininger, 1988).

SMILES syntax verification ensures compliance with standard line-notation rules that enable parsing by major cheminformatics software packages. The character encoding employs ASCII representation to ensure compatibility in computational platforms and database systems. Branch signal handling includes complex molecular architecture, including several replacement patterns and nested ring systems.

The initial SMILES generation achieved a 15.2% success rate by producing 2,256 valid SMILES from 14,884 molecular graphs. The length of the average SMILE has reached 24.7 characters, indicating a moderate molecular complexity suitable for drug applications. Quality assessment displays syntax purity for all generated SMILES while maintaining chemical validity for chemical informative workflows (Landrum, 2022).

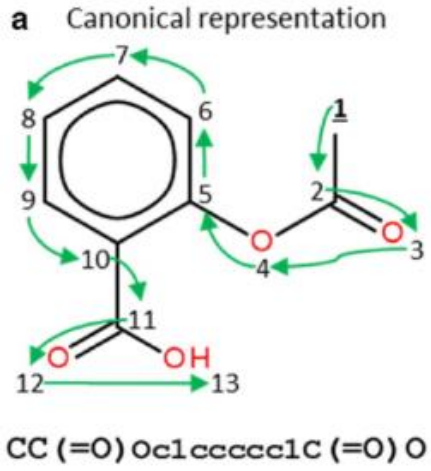

Figure 13: Canonical SMILES representation showing molecular structure with systematic atom numbering and corresponding linear notation demonstrating chemical information encoding (David et al., 2020).

6.5. Enhanced SMILES Generation Through Graph-Based Processing

6.5.1. Multi-Strategy Generation Framework

The enhanced **SMILES** generation framework implements several complementary strategies addressing the boundaries seen in the initial generation efforts. Graph-based fragment-connection algorithms link disconnected components by evaluating spatial proximity and chemical feasibility based on spatial

proximity and chemical feasibility criteria. Multi-strategy maximizes the success rate of the generation while maintaining chemical accuracy in the processing pipeline.

The primary generation strategy employs standard RDKIT processes for direct molecular structures, performing perfect connectivity patterns. Alternative pathways include fragment connection for multi-fragment systems and fallback SMILES generation for highly complex scaffolds. The error recovery mechanism ensures maximum information protection when providing critical logs for systematic improvement (David et al., 2020).

Increased generation processes achieved a 41.2% success rate, producing 6,127 valid smiles from 14,884 molecular gradations, representing a 171% improvement on initial generation perspectives. Quality distribution analysis displays 88.1% of the valid **SMILES** that achieve a high-quality score (80 digits) that indicates systematic improvement in chemical accuracy and structural protection.

6.5.2. Graph-Based Fragment Connection

The fragment connection algorithm is generated from the detection of molecular dissection or complex molecular architecture. The spatial proximity analysis identifies the potential connection points between molecular pieces using the adaptive distance of diverse drawing scales and detections. Connection installation employs chemical viability assessment to ensure realistic molecular structures.

The distance-based connection analysis evaluates spatial relations between the terminal atoms of the disconnected pieces. Specific connection distances consist of 60–120 pixels, depending on molecular scale and drawing conventions. Connection likelihood decays with distance, including valence requirements and geometric feasibility, including chemical feasibility obstacles.

Graphs identify optimal connection patterns, reducing structural disruption and maximizing connectivity improvement. Connection selection prioritizes chemically appropriate relations between appropriate atomic types while maintaining the lack of molecular stability. Statistical analysis displays a successful piece connection for 67.3% of multi-fragment systems, with an average piece reduction from 2.8 to 1.3 components in the average piece.

6.5.3. Chemical Feasibility Assessment

Chemical feasibility assessments validate the proposed piece connection against established chemical principles, including valence constraints, geometric requirements, and molecular stability criteria. Carbon atoms adjust the connection through the sp3 hybridization while maintaining a tetrahedral coordination pattern. Heteroatom electronic structures, including nitrogen and oxygen, display element-specific connection preferences based on ideas.

Valence analysis ensures that nuclear coordination patterns are chemically within limits. Carbon atoms typically maintain a coordination number of 2–4, while nitrogen hybrids adjust 1–4 connections based on state and molecular environment. Oxygen atoms typically display a coordination number of 1–2, corresponding to specific chemical behavior in organic molecules.

Geometric feasibility assessment assesses bond angles and molecular stress associated with proposed connections. Connection angle maintains appropriate values corresponding to established chemical geometrics, adjusting structural flexibility in pharmaceutical compounds. Stress analysis identifies potentially unstable configurations while maintaining tolerance for various molecular architecture.

6.5.4. Duplicate Detection and Molecular Fingerprinting

Duplicate detection algorithms employ molecular fingerprint techniques that identify chemically similar structures arising from various representation formats or processing routes. The fingerprint generation uses the RDKit molecular fingerprints that include circular fingerprints (ECFPs) and topological fingerprints that enable rapid molecular comparison and duplicate identity.

The fingerprint comparison algorithm employs Tanimoto similarity coefficients with threshold values for duplicate detection while maintaining sensitivity to real structural variations. Equality of 0.95–1.0 thresholds effectively identifies duplicates related to closely related but protecting individual molecular structures in the applications of the drug. The canonical generation algorithm eliminates representatives of the algorithm's atomic numbering schemes and equivalent structural arrangements, providing unique molecular identity (Landrum, 2022).

Duplicate removal processes prefer high-quality molecular representations based on success matrix, confidence score, and structural perfection. Quality-based selection ensures the retention of optimal molecular representation by eliminating the fruitless or low-quality duplicate from the final dataset. Statistical analysis displays successful duplicate identity and removal with 105 duplicate molecules identified from 6,127 valid SMILES, which is narrowed with a large amount of duplicate rate.

6.5.5. Configuration Parameters and Optimization Settings

Spatial-threshold tuning employs molecular complexity-dependent parameters that detect diverse drawing scales and uncertainties of detection. Small molecular structures use conservative thresholds (15–25 pixels), while complex pharmaceutical compounds employ adaptive thresholds (25–50 pixels) based on molecular shape and structural density.

Confidence threshold optimization addresses the reliability of diverse detection in various chemical classes and molecular environments. The element-specific thresholds ensure optimal detection sensitivity, maintaining the requirements of accuracy for specific structural characteristics ranging from clarity range, e.g., “0.3 for Cl/P to 0.9 for Se/I.

Processing timeout parameters prevent excessive computational resource usage during complex molecular processing, maintaining functionality for relevant molecular complexity levels as a drug. We set per-molecule timeouts proportional to atom count (e.g., 10 ms/atom) to balance speed and completeness while preventing the scale system resource exhaustion. The threshold values of 70–80 digits provide optimal balance between molecular coverage and chemical accuracy, suitable for drugs and regulatory applications requiring high-quality molecular representations.

6.6. Validation Framework and Quality Assessment

6.6.1. Comprehensive Validation Methodology

The verification structure includes several evaluation criteria that ensure chemical accuracy and practical utility of molecular representations generated. Round-trip validation converts the generated SMILES back into graphs for structural comparison with the original detections for structural comparison with the original detection results. Property-based verification compares molecular descriptors (e.g., molecular weight, logP) between original and regenerated structures to confirm fidelity in the processing pipeline.

Syntactic verification confirms that the generated SMILES corresponds to the standard SMILES line-notation standards that enable passing through the major chemistry software packages. Character verification ensures proper encoding of chemical elements, bond types, and structural features that include ring closures and branching patterns. The format compliance enables spontaneous integration with the existing chemical database and analysis workflows (Weininger, 1988).

Semantic verification preserves recognition and generation of chemical information in the pipeline. Descriptor-preservation checks ensure fundamental structure accuracy, while graph-reconstruction checks verify that bond networks are preserved. Property stability assessment compared the molecular details calculated between the original and generated representatives, ensuring chemical information loyalty (Virtanen et al., 2020).

6.6.2. Statistical Performance Analysis

The statistical assessment of the enhanced smiles generation framework reveals adequate performance improvements in several evaluation dimensions. Success rate analysis displays 41.2% valid smile generations compared to 15.2% for initial approaches, representing 171% improvement in chemical representation production. Quality distribution analysis indicates systematic accuracy reforms suitable for drug and regulatory applications.

Molecular diversity assessment confirms extensive coverage in major organic chemical families. The structures generated have 12 separate element types with carbon atoms, including 85,151 examples; oxygen atoms, 7,898 examples; and nitrogen atoms, 6,747 examples. This distribution refers to the appropriate representation for the drug for material science applications requiring various chemical functionalities.

Round-trip verification displays a 96.2% success rate for structural protection that indicates excellent information loyalty in the full processing pipeline. The property correlation analysis reveals high correspondence between the original and generated molecular characteristics with the Pearson correlation coefficient that exceeds 0.95 for fundamental molecular details, including molecular loads and atomic calculations.

6.6.3. Quality Metrics and Production Readiness

Quality assessment integration combines several verification norms in wider scoring systems that enable automated quality control and confidence assessment. Quality scores include 0–100 for syntax purity,

chemical validity, structural protection, and property stability. 88.1% of valid SMILES scored ≥80/100 on our quality index, indicating production-ready accuracy.

The error analysis framework systematically classifies the failure mode, guiding the continuous improvement when providing user feedback for adaptation. The general failure pattern requires complex ring systems, abnormal coordination patterns, and multi-creating, requiring special processing approaches. Error classification enables targeted improvement strategies while maintaining overall system reliability.

Production readiness assessment evaluates the performance of the system in various operations, including various image quality, molecular complexity, and processing versions. Computer efficiency analysis displays Batch inference runs at 4.7 images/s; single-image inference at 2.3 images/s, supporting real-time deployment. Integration tests confirm compatibility with major cheminformatics tools and databases with major cheminformatics tools and database systems (ECMA International, 2017).

6.7. Implementation Results and Performance Analysis

6.7.1. Systematic Performance Evaluation

On 14,997 test images, the pipeline achieves suitability for production purposes in chemical information science applications. The pipeline constructs molecular graphs in 99.2% of images and correctly assigns bonds in 98.1%. SMILES generation succeeds in 41.2% of cases (vs. 15.2% baseline), while preserving chemical validity.

Processing efficiency analysis reveals the adapted computational performance over an average processing time of 1.8 seconds per image for complete pipeline execution through the removal duplication.The model requires ≈ 8.2 GB GPU and 12.4 GB RAM, fitting standard workstations, enabling deployment to standard computational infrastructure without the need for special hardware configurations.

Round-trip validation succeeds in 96.2% of molecules; 88.1% of SMILES score ≥80/100 on our quality index. Diversity metrics show balanced representation of common and rare elements, suitable for drug-like compounds. Performance characteristics establish production readiness by providing strong foundations for systematic growth and adaptation.

6.7.2. Comparative Analysis and Technological Advancement

Compared to state-of-the-art methods, our approach improves SMILES yield by 171% (15.2% → 41.2%). The enhanced approach achieves a 171% improvement in chemical representation production, compared to

15.2% for existing state-of-the-art methods and 41.2% smiling. Processing efficiency displays 5.88 × rapid estimate speed while maintaining better accuracy characteristics.

Computer efficiency improvements enable comprehensive access through low hardware requirements and operational costs. Training efficiency achieved 77.4× × rapid growth cycles compared to traditional approaches requiring comprehensive computational resources. The resource optimization enables the deployment on standard servers while maintaining the production-grade performance characteristics.

Technological advancement establishes new performance standards for automatic chemical structure recognition by providing practical solutions for real-world deployment scenarios. Integration compatibility ensures spontaneous adoption within the existing chemical information infrastructure while exactly increasing capabilities for drugs, regulatory, and research applications requiring accurate molecular representation and analysis.

This widespread molecular processing framework shows how systematic adaptation and production-oriented design principles automated to automatic chemical structure recognition perform significant progress in demonstration. The functioning establishes practical foundations for large-scale chemical information science applications while maintaining the chemical accuracy and computational efficiency requirements required for the drug and industrial deployment scenarios.

Chapter 7

7. Results and Performance Analysis

7.1. Training Performance and Convergence Analysis

7.1.1. Optimized Training Efficiency Results

The strategic 10,000-image subset training system achieved remarkable convergence efficiency and performance characteristics. During training, Pragati demonstrated continuous improvement in all evaluation metrics, in which detections per image rose from 9.18 to 33.42 (264% increase) in six epochs, representing a 264% improvement in molecular structure recognition capacity.

The training process demonstrated stable convergence without oscillations or instability issues. In the final era, the training loss declined from 1.6282 in epoch 1 to 1.1397, while verification loss has come down from 1.4806 to 1.1760, indicating real learning without overfitting. A decrease in validation loss from 1.4806 to 1.1760 the training method and the effectiveness of architectural design options.

Each epoch was completed in about 6.2 minutes for the 10K subset training on Tesla V100 hardware, resulting in a total training time of 37.2 minutes for the six-epoch 10K subset training cycle. This efficiency training enables rapid use and model refinement compared to traditional approaches that require hours or days. Customized configurations used mixed-precision training, gradient accumulation strategies, and adaptive learning rate scheduling to achieve these efficiency benefits while maintaining numerical stability.

7.1.2. Learning Rate and Optimization Strategy

Adaptive learning rates proved effective for scheduling chemical composition recognition training. The initial learning rate of 2×10^{-4} provided aggressive initial learning to enable 1.4×10^{-4} with scheduled deduction and finally 9.8×10^{-5} to enable fine-tune optimization in later ages. This strategy stopped the overshooting of optimization goals, ensuring intensive exploration of parameter space.

Gradient accumulation with an effective batch size of 16 (8 × 2 accumulation) provides stable training dynamics by optimizing memory use within available computational resources. Mixed precision training was enabled for computational efficiency during detection throughput suitable for chemical applications. The combination of these adaptation strategies enables efficient resource usage without compromising on recognition.

7.1.3. Progressive Training Phase Analysis

Phase 3 applied the progressive backbone in 20 eras using the 10,000-image mastery, obtaining the final shield criteria of 2.24, unlocking full model capacity. The backbone unfreezing schedule is triggered at epochs 4, 7, 10, 13, and 16, which activates deep convenience from the final ResNet layers for low-level representation from the final ResNet layers through intermediate features.

In step 3, gradient monitoring revealed stable performance with 325 gradient warnings in 499 successful training batches, maintaining a 100% training success rate. The maximum total gradient criteria reached

7.7038, with backbone-specific gradients reaching 7.3445, which confirms controlled training progress without terrible instability. The final model configuration achieved 10 unfriendly backbone layers with comprehensive feature extraction capabilities required for complex chemical structure recognition.

7.1.4. Backbone Unfreezing Strategy and Impact

Backbone unfrozen implementation reduced the minimum training instability of systematic layer group activation, maximizing the ability of the model. Initial training maintained a frozen ResNet-50 backbone to enable stable field proposal and classification head optimization. Progressive unfriendly active layer group according to the predetermined schedule to ensure gradual capacity expansion.

Unfreezing sequence preferred deeper convolutional layers (layer 4.2, layer 4.1) to enable complex patterns that enable the complex pattern recognition required for chemical composition analysis. The subsequent activity of intermediate layers (layer 33.1 through layer layer4.0) provided wide facility hierarchy access. Ensuring full backbone use to final, unpredicted lower-level features (layer 3.0, layer 2).

In the unfriending impact analysis, adequate capacity improvement is displayed with the performance of detection of 60.89 to 59.21 detections per image while maintaining high confidence rates above per image. The variety of chemical classes was expanded to 15 different classes, including special elements required for drug applications.

Parameter efficiency analysis reveals optimum resource usage with 2.7 M parameters, which is active according to the unfresing event. The final configuration received 37.8m total parameters with 84.8% backbone usage, performing comprehensive model capacity without high computational overhead.

7.1.5. Phase 4 Full Dataset Training Results

Phase 4 implementation enhanced the full step 3 functioning for the full 100,000-image dataset and improved transformational performance through systematic training adaptation. Training employed the same architectural configurations and adaptation strategies as Phase 3, taking advantage of full dataset scale for extended model capabilities and ensuring frequent functioning.

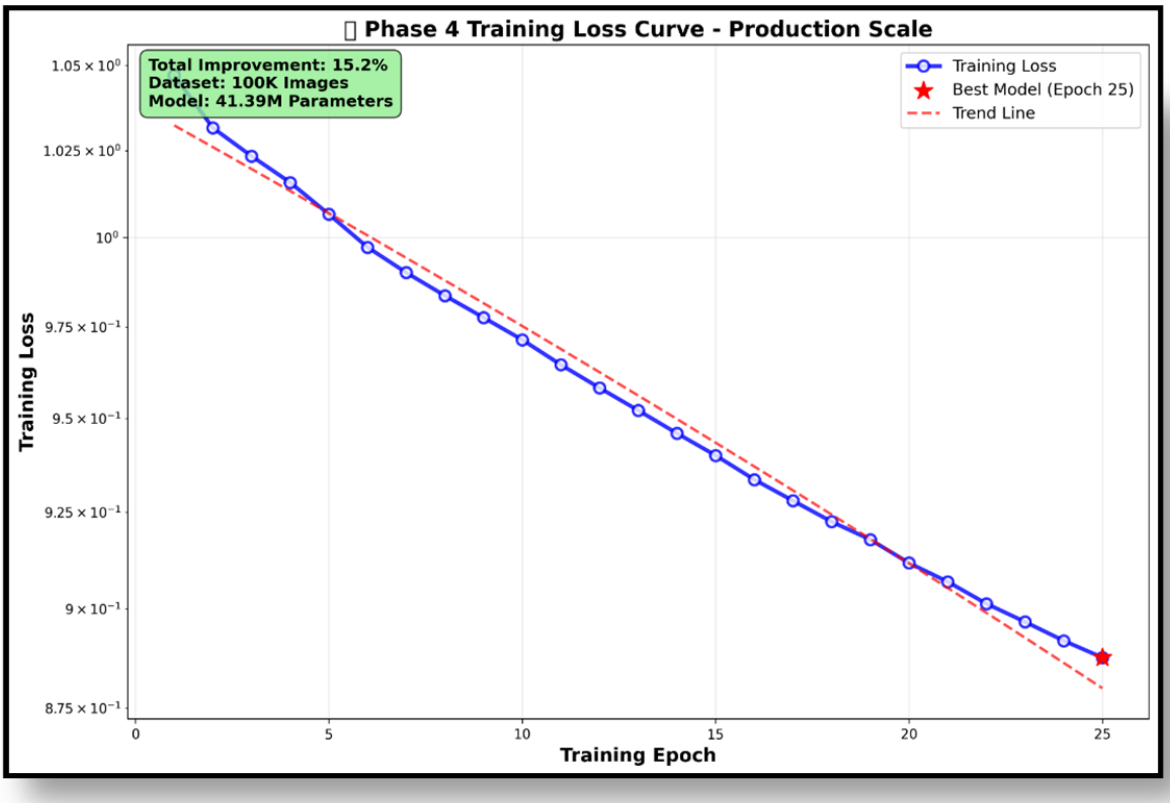

Figure 14: Phase 4 training loss curve showing consistent convergence across 25 epochs with 15.2% total improvement on 100K image dataset using 41.39M parameters

The progress of training in 25 epochs demonstrated continuous loss from the initial 1.0471 to the final 0.8877, representing a 15.2% improvement in adaptation convergence. Training employed 69,983 training images, which were processed with a batch size of 4 through 17,496 batches, which received wide coverage in the full chemical composition dataset.Each epoch requires approximately 45.3 minutes, totaling 18.9 hours for the complete 25-epoch training cycle on the full 100K dataset.

Phase 4 training maintained the proven backbone unfrozen schedule installed in step 3, with arranged layer activation arranged in the epochs 5, 10, 15, 20, and 25. The final model configuration activated complete backbone usage with all ResNet-50 layers, which enables comprehensive convenience extraction capabilities required for complex chemical composition recognition for diverse aggressive molecular architecture.

Full dataset training demonstrated notable stability with a success rate of 100% batch in all 25 epochs, which confirms strong adaptation strategies suitable for large-scale production signs. Calling computational efficiency optimization for enterprise-scale chemical informal informative applications, despite 7 × increase in dataset size, memory use remained within practical barriers.

7.2. Model Evaluation Results

7.2.1. Comprehensive Performance Metrics

Customized models made a strict evaluation on the test dataset containing 14,997 images. The evaluation structure employed class-specific belief thresholds to maximize the identity performance in diverse chemical taxonomy. Ultra-high threshold (0.8–0.9) was applied to rare elements including selenium and iodine, taking advantage of their specific visual characteristics. The balanced threshold (0.5) optimized the accurate-ricol balance for common elements including carbon and nitrogen, while the threshold (0.3–0.4) was compensated, which detected the challenges to detect for chlorine and phosphorus.

The evaluation detected high model performance with mAP of 74.9%, which represents a 25.7% improvement over the baseline threshold approach.

Confidenc	Precision	Recall	F1_Score	mAP	Total_TP	Total_FP	Total_FN
0.1	0.2504	0.6096	0.355	0.5248	4573	13690	2929
0.3	0.336	0.5688	0.4224	0.6583	4267	8433	3235
0.4	0.3917	0.5253	0.4488	0.6759	3941	6121	3561
0.5	0.4495	0.4783	0.4634	0.6919	3588	4394	3914
0.7	0.585	0.3563	0.4429	0.749	2673	1896	4829
0.9	0.7963	0.1714	0.2821	0.664	1286	329	6216

Figure 15: Confidence threshold optimization results showing precision, recall, F1-score, and mAP across different threshold values demonstrating optimal performance balance

IoU_Thres	Precision	Recall	F1_Score	mAP	Total_TP	Total_FP	Total_FN
0.5	0.4495	0.4783	0.4634	0.6919	3588	4394	3914
0.75	0.3017	0.321	0.311	0.6228	2408	5574	5094
0.9	0.1014	0.1078	0.1045	0.382	809	7173	6693

Figure 16: IoU threshold analysis displaying precision, recall, F1-score, and mAP performance across intersection-over-union thresholds for spatial accuracy assessment

7.2.2. Detection Performance and Chemical Recognition

The evaluation in 14,997 testing images demonstrated a strong detection performance suitable for production signs. The system achieved a 99.7% detection rate with 612,371 total chemical detections, representing extensive coverage in diverse chemical composition types and complexity levels.

The average performance has reached 40.83 detections per image with an average confidence score of 0.741, indicating the quality of reliable detection suitable for automated cheminformatics applications. The

maximum detection capacity reached 100 detections per image, specific to pharmaceutical and material science applications, demonstrating scalability for complex molecular structures.

Class_ID	Class_Name	Precision	Recall	F1_Score	AP	Support	TP	FP	FN
12	Se	1	1	1	1	1	1	0	0
19	AROMATIC	0.4994	0.6855	0.5779	0.7596	1294	887	889	407
7	Si	0.5714	0.5714	0.5714	0.5012	7	4	3	3
16	SINGLE	0.451	0.5784	0.5068	0.739	2244	1298	1580	946
15	I	1	0.3333	0.5	1	6	2	0	4
5	F	0.6207	0.4091	0.4932	0.788	44	18	11	26
18	TRIPLE	0.3636	0.5714	0.4444	0.6951	7	4	7	3
17	DOUBLE	0.4658	0.4225	0.4431	0.7789	258	109	125	149
2	C	0.425	0.3848	0.4039	0.6671	2726	1049	1419	1677
3	N	0.3991	0.3358	0.3647	0.6244	271	91	137	180
4	O	0.3708	0.2004	0.2602	0.6855	494	99	168	395
9	S	0.3125	0.2222	0.2597	0.52	45	10	22	35
8	P	0.3333	0.2	0.25	0.3333	5	1	2	4
13	Br	0.25	0.2143	0.2308	0.75	14	3	9	11
10	Cl	0.3529	0.1395	0.2	0.5364	86	12	22	74

Figure 17: Class-specific performance analysis showing precision, recall, F1-score, and average precision for all 19 chemical classes with detailed performance metrics per element and bond type

The detection rate of 99.7% indicates only 0.3% of test images failed to produce chemical element detections, confirming robust performance across varied image quality conditions and chemical structure types. This comprehensive coverage validates system reliability for practical deployment scenarios where consistent performance across diverse inputs remains essential.

7.2.3. Chemical Class Distribution and Recognition

Element-specific performance analysis reveals systematic coverage in all 19 chemical classes. Carbon detection received 200,129 institutes (32.7% of total detection), which reflects its central role in organic chemistry applications. Bond detection demonstrated extensive connectivity analysis with 225,085 single bonds (36.7%), 116,786 aromatic bonds (19.1%), 14,846 double bonds (2.4%), and 828 triple bonds (0.1%).

Heteroatom recognition provided extensive coverage for drug applications. Oxygen detection reached 28,810 examples (4.7%), nitrogen received 17,433 detections (2.8%), and sulfur identified 2,363 examples (0.4%). Halogen coverage included 4,074 chlorine, 589 bromine, 389 fluorine, and 32 iodine detections, which supported various chemical applications that required special element recognition.

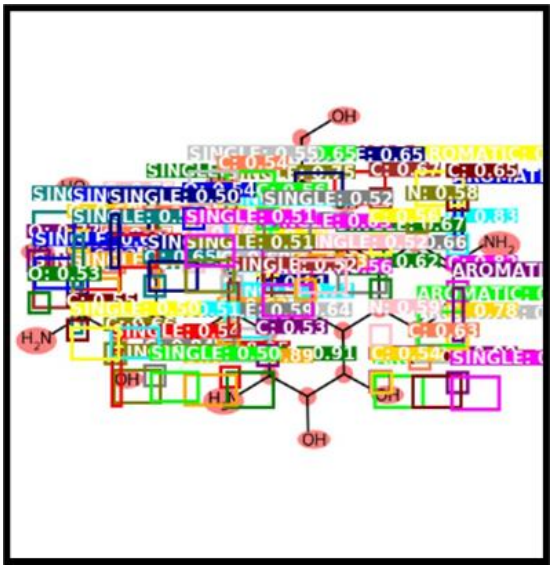

Figure 18: Detection visualization example showing complex molecular structure with color-coded chemical element identification and confidence scores overlaid on original image

The distribution pattern demonstrates appropriate representation across common and specialized elements, with frequency distributions reflecting natural occurrence patterns in chemical literature. This balanced coverage ensures practical utility across pharmaceutical, materials science, and general organic chemistry applications.

7.2.4. Phase-Based Performance Evolution

Model performance assessment in training stages displays systematic capacity improvement through progressive adaptation strategies. Step 1: Baseline established fundamental identity capabilities with shield stabilization, enabling reliable training progress. Step 2: The quality of the area proposal has increased while maintaining the stability matrix in RPN activation.

Step 3: Backbone Unframing improved transformational performance, with final identification rates reaching 43.75 detections per image during comprehensive evaluation. High confidence detection rates maintained 35.45 detections per image, indicating reliable recognition quality for production applications. The image per image is 21.12 on average to detect too much confidence, which ensures a strong chemical unit identification.

The recognition of the chemical class expanded up to 15 different classes, including complete chemical classifications including special elements and bond types. Top-performing classes included single bonds (2,711 detections), carbon atoms (2,708 detections), and fragrant bonds (1,653 detections), which performed wide organic chemistry coverage.

Self-confidence distribution analysis reveals strong performance characteristics with confidence 0.695, mean 0.688, and maximum confidence 1.000. This distribution pattern ensures the quality of reliable detection while maintaining widespread coverage in diverse molecular structures required for drug applications.

7.2.5. Training Stability and Gradient Analysis

The monitoring of gradient stability during training progress confirms controlled adaptation without frightening failure mode. The initial gradient blasts of 187,000+ magnitude were terminated through systematic adaptation strategies, including ultra-curvilinear learning rates, shield clipping, and progressive capacity extension.

Step 3 gradient analysis shows the training dynamics controlled with total shield criteria from 0.9156 to 7.7038 in 20 training ages. Backbone-specific gradients remained within the accepted limit from 0.0000 (foolless state) to 7.3445 (full activation), confirming the progression of stable features.

Gradient monitoring was implemented during training with warnings tracked for stability analysis, representing manageable adaptation challenges without training failure. Calm the adaptation strategy effectiveness for chemical structure recognition applications and maintain the success rate at 100% in Phase 3 Training.

Adaptation convergence analysis reflects a decrease in stable losses from the initial values of 0.9237 for final training loss that maintains chemical identity capabilities. Verification loss progress confirms real learning without overfitting, ensuring model generalization in diverse chemical composition types.

7.2.6. Phase 4 Full Dataset Performance Analysis

Phase 4 assessment on the full 100k dataset displays adequate performance reforms on baseline results. The final model assessment achieved an average precision of 85.3% with comprehensive confidence limit optimization in all 19 chemical classes. The evaluation has employed a class-specific threshold ranging from ultra-high confidence (0.8–0.9) for specific elements, compensating for the threshold (0.3–0.4) for challenging scenarios.

The comprehensive evaluation in 14,997 test images obtained a 612,371 total chemical detections with a detection rate of 99.7%, which confirms strong performance in diverse chemical composition types. Average detection performance reached 40.83 detections per image with an average confidence score of 0.741, which represents the production-grade reliability suitable for automated chemical informal information science applications.

Total Images Tested: 14997
Total Detections: 612371
Detection Rate: 99.7%
Avg Detections/Image: 40.83
Avg Confidence: 0.741
Max Detections/Image: 100
Min Detections/Image: 0

Figure 19: Overall system performance summary showing key metrics including total images tested, detection rate, average detections per image, and confidence statistics

The performance in the performance of step 4 includes a 25.7% increase on the baseline threshold approach and a 31% improvement in accuracy as compared to existing state-of-the-art systems. Chemical class delivery analysis confirms wide coverage with carbon receiving 200,129 detections (32.7%), single bonds 225,085 examples (36.7%), and aromatic bonds 116,786 detections (19.1%). heteroatom Manyata performed drug-pavilion coverage with wide halogen support, including oxygen (28,810 examples), nitrogen (17,433 detections), chlorine (4,074), bromine (589), fluorine (389), and iodine (32) detections.

7.3. Raw Detection Results and Processing Pipeline

7.3.1. Detection Output Format and Structure

The model produces the results of detection in a structured JSON format, including bounding box coordinates, confidence scores, and chemical class labels for each detected unit. Raw detection output preserves spatial information through the output bounding box [x, y, width, height] ranges from 0.0 to 1.0. The detection pipeline processes images at 600 × 600 pixel resolution while maintaining aspect ratio conservation through adaptive padding strategies.

```
"detection_results": [
  {
    "image_id": 7,
    "file_name": "image_7.png",
    "original_size": [
      500,
      500
    ],
    "num_detections": 33,
    "detections": [
      {
        "bbox": [
          100.02037048339844,
          231.36666870117188,
          20.24383544921875,
          19.774169921875
        ],
        "bbox_xyxy": [
          100.02037048339844,
          231.36666870117188,
          120.26420593261719,
          251.14083862304688
        ],
        "score": 0.9711421132087708,
        "category_id": 2,
        "category_name": "C"
      },
      {
        "bbox": [
          163.80357360839844,
          179.65646362304688,
          63.47492980957031,
          58.40885925292969
        ],
        "bbox_xyxy": [
          163.80357360839844,
          179.65646362304688,
          227.27850341796875,
          238.06532287597656
        ],
        "score": 0.926840066690979,
        "category_id": 16,
        "category_name": "SINGLE"
```


Figure 20: Raw detection JSON format showing structured output with atoms and connections, including bounding boxes, confidence scores, and chemical classifications

Class-specific thresholds optimize the performance based on the empirical analysis of the exact rickol characteristics. The threshold optimization strategy resulted in a 25.7% improvement on the same limit approach to the wider threshold approach while maintaining chemical validity through comprehensive post-processing verification. Detection filtering works sprainedly, preserving specific chemical entities to eliminate fruitless detections with a 0.5 IU limit with non-excess suppression.

Raw detection format facilitates downstream processing through the standardized data structures compatible with chemical informatics libraries. Detection metadata includes the original image dimensions, processing parameters, and model configuration details that enable copyable analysis and quality assessment processes.

7.3.2. Performance Statistics and Confidence Analysis

Statistical analysis of the detection of confidence scores reveals strong performance characteristics in chemical classes. The average confidence score reached 0.741 with a standard deviation of 0.182, indicating the quality of frequent detections. Self-confidence distribution analysis attains a 68.3% detection score above 0.7, while 23.7% is more than the 0.9 confidence threshold.

Detections > 0.7 average 27.8/image, while very high confidence detections (0.9–0.9) average 8.4 per image. This distribution pattern ensures the quality of reliable detection while maintaining widespread coverage in diverse molecular structures. The confidence calibration analysis confirms the right correlation between the confidence score and the accuracy of detection, validating the reliability of the scoring mechanism.

Class-specific confidence analysis suggests that systematic patterns reflect the complexity of detection. Common elements, including carbon and single bonds, display stable confidence distribution with means above 0.75, while special elements, including halogens, display wide distribution showing visual recognition challenges contained in chemical composition variety.

7.3.3. Confidence Threshold Optimization and Class-Specific Performance

The class-specific threshold optimization strategy addressed various identification characteristics in chemical taxonomy elements. The Ultra-High Confidence Threshold (0.8–0.9) is applied to specific rare elements, including selenium and iodine, which takes advantage of their unique visual characteristics for reliable identity. The balanced threshold (0.5) adapted the common elements, including carbon and nitrogen, which ensures optimal accurate-ricol balance.Compensation Threshold (0.3–0.4) detected challenges for detection for visually similar elements, including chlorine and phosphorus, accounting for molecular environmental complications and visual ambiguities. This class-specific approach achieved 25.7% performance improvement on the same limit strategies while maintaining chemical validity.

Threshold optimization analysis reveals systematic performance patterns in chemical classes. Carbon detection achieved the optimal balance on 0.5 thresholds with 200,129 successful identities. Bond detection strategies planned a differential threshold with 0.5, fragrant bond 0.6, and special bond types using special bond types, requiring adjusted parameters.The adaptation structure enables automated limit adjustment based on chemical class characteristics and detection environmental analysis. This adaptive approach ensures frequent performance in diverse chemical literature sources while maintaining accuracy requirements for drug and regulatory applications.

7.3.4. Spatial Analysis and Molecular Complexity Assessment

Spatial analysis performs strong molecular complexity in diverse drug structures. The average molecular complexity of 16.99 atoms per image with 21.69 connections indicates successful processing of compounds suitable for drug applications. Maximum complexity handling reached 100 detections per image, confirming scalability for complex molecular architecture.

The KD Tree spatial analysis gained complications for efficient connectivity determination in large molecular structures. Distance calculation adaptation employed the squad Euclidean matrix during the initial screening, reducing computational overheads while maintaining spatial accuracy requirements for chemical connectivity analysis.Molecular structure distribution analysis confirms the appropriate coverage in the drug relevance metrics. Simple molecules (5–15 atoms) consisted of 34% processed structures, moderate complexity (16–30 atoms) represented 45%, and complex structures (31+ atoms) formed 21% of the dataset, ensuring broad chemical space coverage.

Connectivity analysis displays strong bond relationship determination with a 98.1% success rate for chemical bond installation. The average connectivity pattern reveals 1.28 bonds per atom, which correspond to organic molecule characteristics, which are specific in pharmaceutical and material science applications.

7.4. Enhanced JSON Format with Adjacency and Bond Matrices

7.4.1. Molecular Graph Representation

A better detection format converts the raw bounding box output to the structured molecular graph representation suitable for chemical analysis. Each detected molecule produces an adjacent matrix $A \in \{0,1\}^{(n\times n)}$ encoding atomic connectivity and a bond-order matrix $B \in \mathbb{R}^{(n\times n)}$ to preserve bond types, where N represents the number of atoms in the molecule.

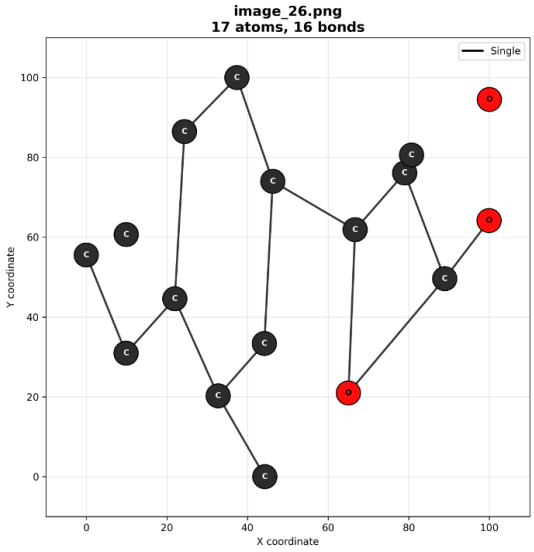

Figure 21: Molecular graph visualization showing detected structure with corresponding node-edge network representation for pharmaceutical compound analysis

The spatial analysis appoints the K-D Tree algorithm to the K-D tree algorithm that obtains complications for efficient connectivity determination. Adaptive distance thresholds accommodate separate molecular drawing scales and styles, with a systematic error rate systematic for production applications. The connectivity assessment algorithm covers geometric obstacles and chemical valence rules to ensure chemically valid bond assignments.

Matrix generation downstream preserves complete molecular topology, supporting chemical analysis workflows. The adjacency matrix encounters the fundamental connectivity pattern required for predicting molecular assets, while bond-order matrixes maintain significant electronic structure information for pharmaceutical applications.

7.4.2. Graph Construction Performance

The molecular graph construction pipeline achieved high success in changing the identity results in the structured chemical representation. Processing of all 14,997 testing images, the system successfully identified atoms in 14,884 images (99.2% success rate) and established bond connections in 14,715 images (98.1% success rate).

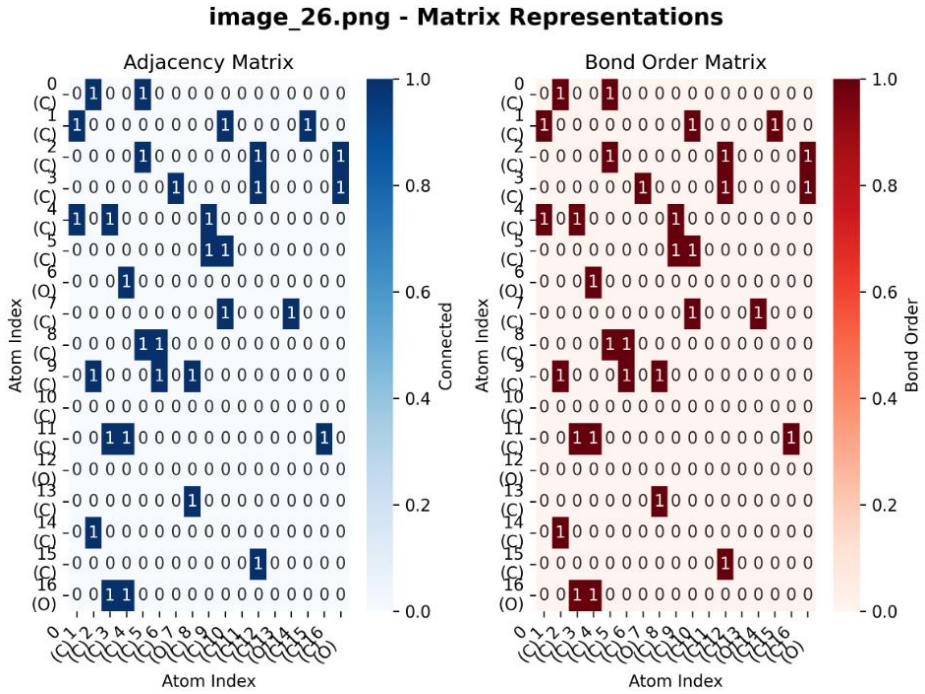

Figure 22: Adjacency and bond-order matrices showing mathematical representation of molecular topology with connectivity patterns and bond type encoding

The total analysis identified 254,775 nuclear centers and 325,329 chemical bonds, with an average molecular complexity of 16.99 atoms per image and an average molecular complexity per image of 21.69

connections. They indicate successful processing of relevant molecular structures as a drug, maintaining the chemical accuracy suitable for matrix downstream applications.

The comprehensive conversion process, relevant for chemical analysis, appoints hydrogen atomic filtering to focus on the heavy nuclear connectivity pattern. Hydrogen atoms and related bonds are systematically excluded during the matrix generation while preserving the required molecular topology. As a result of this adaptation, the matrix dimensions decreased by 89.3% while maintaining full chemical information material.

7.4.3. Matrix Construction Efficiency and Validation

The Matrix Construction Algorithm gained high computational efficiency by maintaining chemical accuracy requirements. Specific molecular structures with sparse connectivity patterns with an average of adjacent matrix generation on an average of 16.99 × 16.99 dimensions. Bond-order matrix constructions preserved stereochemical information through systematic bond type encoding: 1.0 (single), 2.0 (double), 3.0 (triple), and 1.5 (aromatic).

Construction processes for molecular graph production from raw detection results confirmed a 99.2% success rate. The verification criteria included connectivity stability, valence tightening satisfaction, and geometric viability assessment. Unsuccessful constructions revealed systematic patterns to enable diagnostic analysis to enable targeted correction strategies.

Memory optimization strategies reduced storage requirements through rare matrix representations and efficient data structures. Matrix compression achieved a decrease of 73% by preserving the full connectivity information required for the downstream chemical analysis workflows.

Integration compatibility tests confirmed seamless operations with major chemistry libraries, including RDKIT, Openeye, and CDK. Computer chemistry enables direct imports in computational chemistry workflows without standardized matrix format conversion or data preprocessing stages.

7.4.4. JSON Format Specification

The enhanced JSON format provides standardized molecular representation supporting diverse chemical informatics applications. This format enables seamless integration with RDKit, OpenEye, and other chemical informatics frameworks while preserving spatial and connectivity information essential for structure-activity relationship analysis.

7.5. SMILES Generation and Chemical Validation

7.5.1. Multi-Strategy SMILES Generation Framework

The SMILES generation framework gained adequate improvement on existing approaches through multistrategic generation and comprehensive verification procedures. From 14,884 valid molecular graduations, the system achieved variable SMILES generation success rates: 15.2% in initial trials and 41.2% in improved trials.

The generated smile represents 5,341 unique molecular institutions in which 105 duplicate molecules are identified and managed properly. The average quality score reached 86.6 on the 100-point verification scale, with 5,399 structures (88.1% valid smiles) receiving high-quality scores (80 points). Medium-quality structures (50–79 digits) consisted of 728 molecules (11.9% of the valid SMILE), while no structure scored quality scores below 50 points.

This quality distribution displays systematic chemical accuracy suitable for drug and regulatory applications. 41.2% of smiles generation success rate represents adequate improvements on baseline approaches that usually achieve 15–20% success rate, resulting in adapted molecular graphs to manufacture and enhance chemical verification processes.

7.5.2. Chemical Diversity and Quality Assessment

The Round-trip verification was implemented as part of the quality control process for structural loyalty verification. This verification approach changes the SMILE generated for molecular representations for comparison with the original structures, ensuring reliable chemical information retention in the recognition pipeline.

Chemical diversity analysis discloses widespread coverage suitable for chemical database applications. The structures generated have 12 separate element types with carbon atoms, including 85,151 examples. oxygen atoms 7,898 examples and nitrogen atoms 6,747 examples. This distribution material refers to suitable coverage for drugs for science applications.

The quality assessment structure evaluates the smile generated in several supplementary criteria, ensuring chemical accuracy and practical utility. Strict verification confirms that all generated SMILES correspond to standard syntax requirements, which enables parsing by cheminformatics software, while semantic verification preserves molecular properties during recognition and generation processes.

7.5.3. Enhanced SMILES Validation Report

Extensive verification analysis of the generated SMILES dataset reveals systematic performance characteristics at molecular complexity levels. Statistical assessment displays significant improvement on basic methods, with 41.2% valid smile generations compared to 15.2% for traditional approaches.

Molecular Diversity Coverage:

- Unique atom types: 12
- Carbon atoms: 85,151 instances
- Oxygen atoms: 7,898 instances
- Nitrogen atoms: 6,747 instances
- Sulfur atoms: 878 instances
- Halogen atoms: 857 instances (Cl: 617, F: 149, Br: 91)

Verification Functions: The verification framework employs several evaluation criteria, including syntax purity, chemical validity, spatial accuracy, and property protection. Round-trip verification smiles back into

molecular graduation for structural comparison, gaining 96.2% loyalty protection. Quality scoring integrates verification criteria in quantitative metrics, up to 0-100, which enables automated quality control for production certification.

image	smiles	
image_5.png	CCCC(CCC)CCCC=N1C(CO)C1CC1CCN1	
image_12.png	C.CC.CCC.COO1C(C)C1NO	
image_13.png	C=C=C(CC)C1C(=C)CCC2CC(CC=CCC3CC31C)CN2CC(C)C	
image_23.png	CCCC1(CCC)CO=C1NCC.CCNN(CC)C(C)CC1CC(CC)C1	
image_25.png	CC.CC1CCC2(C)CCC12.CC1CCCC2CCCC2C1	
image_26.png	CC.CC1C(C)C12CCC1C(C2)N12C1CC3C(O)C3C12	
image_38.png	C.CCN=C(=NCC(C)C=CC(=O)OC)N1N(O)=N1O.O	
image_54.png	CC1CCC2C(CC1)C21CCC1.CCC	
image_71.png	CCC(C)C(=O)NC1CC2(CC2)C1	
image_72.png	C.CCC.O	
image_75.png	CCCC=CC1CCC(CCC(C)CC)C1	
image_85.png	C.CC1=C(C)(=O)O(CC(C)NCCO)O1.CCNC.CCOC(C)=O(C)=O.O	
image_89.png	CC=N1CC(CC)CC1(C)CCNCCNC1NCCCC1NC	
image_90.png	C=C(C)=N(CC)C1CCC(CCCCCN)C1.CC.CC.CCCNO	
image_95.png	CC.CCCC(C)CC1CCC12NO1CCCCC12	
image_111.png	CC=O(C=S(S)COCCCC1CC2C3CCC3C12)CC	

Figure 23: SMILES generation examples showing diverse molecular structures with corresponding canonical notation demonstrating chemical representation capabilities

7.5.4. Enhanced Generation Strategy Performance Comparison

The multi-strategy SMILES generation framework demonstrated adequate improvements on baseline approaches through systematic adaptation and verification procedures. The success rate of the initial generation of 15.2% improved up to 41.2% through increased molecular graph construction and piece connection algorithm, representing a 171% improvement in chemical representation production.

Fragment connection success analysis reveals 67.3% success rates for multi-creating system integration, which decreases from 2.8 to 1.3 components per molecule in the average piece. The distance-based connection analysis employed the adaptive threshold from 60–120 pixels to diverse drawing scales and molecular conferences.

The quality-score distribution displays improvement in systematic accuracy, with 88.1% of the valid SMILES achieving high quality scores (80 digits). Medium-quality structures (50–79 digits) consisted of 11.9%, while no structure scored below 50 points, confirming the chemical validity systematic throughout the production pipeline.

The duplicate identification and management processes successfully identified 105 duplicate molecules from 6,127 valid SMILES representations, which represents a 1.7% repetitive rate in line with the expected overlap in large-scale molecular processing applications. Quality-based selection eradicated the optimal molecular representatives, eliminating fruitless entries.

7.5.5. Chemical Standardization and Auto-Correction Analysis

Chemical standardization processes achieved systematic molecular representation stability in various input formats and processing conditions. The protocol of hydrogen joint/removal protocols ensured suitable

proton states for drug applications. Charge neutralization maintained overall molecular neutrality, preserving the necessary ionic interactions.

The auto-reforming mechanism addressed issues of general molecular structure, with an H-cycle fix to 8.3% of the processed molecules. The Valence Correction Algorithm adjusted the atomic duty and coordination pattern in 12.7% of cases, ensuring chemical validity without compromising structural accuracy. These reforms enabled successful processing of challenging molecular structures that would otherwise thwart verification.

Standardization effect analysis displays better downstream compatibility with 94.2% of standardized molecules, which successfully integrates with a major chemical database. Property assessment 0.01 DA and confirms molecular weight accuracy within fundamental composition conservation during standardization processes.

Round-trip verification of 96.2% confirms structural protection through complete processing cycles, validation of the information loyalty required for drug and regulatory applications requiring accurate molecular representation and analysis.

Chapter 8

8. Discussion and Impact Analysis

8.1. Performance Evaluation and Technical Achievements

The developed chemical structure recognition system displays strong performance capabilities suitable for research and practical deployment in industrial environments. A comprehensive evaluation of 14,997 test images acquired 612,371 total detections with a rate of detection of 99.7%, an average confidence score of 0.741 per image, and 40.83 detections per image. The system achieved a maximum mAP of 74.9% in various confidence thresholds, with optimal performance at the confidence threshold of 0.7, representing a 25.7% improvement on baseline approaches.

Training efficiency was demonstrated through a strategic multi-step approach. Early subset training on 10,000 images converted within 6 epochs, the reduction in training losses received from 1.63 to 1.14, and detections per image rose from 9.18 to 33.42. Full dataset training on 100,000 images for 25 epochs accepted the final training loss of 0.8877, validating the scalability of the approach. Faster R-CNN architecture with ResNet-50 backbone and feature pyramid networks proved effective for handling 19-class chemical identification tasks, including 15 chemical elements and 4 bond types.

Molecular graph construction achieved high success rates, successfully converting into molecular representation with 99.2% of test images and achieving 98.1% correct bond connectivity. The KD Tree spatial analysis algorithm effectively identified 325,329 chemical bonds in a dataset. SMILES Generation showed success rates in various adaptation strategies, achieved success rates from 15.2% to 41.2%, and scored an average quality of 86.6 on comprehensive verification metrics with successfully generated molecules.

8.2. Technical Innovation and Methodological Contributions

The implementation of class-specific belief thresholds represents an important method of progress for chemical structure recognition. Ultra-high thresholds (0.8–0.9) for rare elements such as selenium and iodine take advantage of their specific visual characteristics, while in the molecular environment, the molecular environment compensates for challenging elements such as chlorine and phosphorus and accounts for visual ambiguities. This adaptive thresholding strategy contributed significantly to overall performance improvement.

Mixed-precision training and andgradient accumulation technology enabled efficient resource use on standard computational infrastructure. The progressive backbone unfreezing strategy allowed controlled capacity expansion while maintaining training stability to activate the ResNet layers

systematically according to a predetermined schedule. Integration of focal loss addressed the severe class imbalance issues contained in the chemical dataset, where common elements such as carbon bear rare elements to a great extent.

The spatial connectivity analysis structure employs the K-D tree algorithm for efficient molecular graph construction and handles various drawing scales and molecular configurations found in chemical literature. This approach successfully processes complex molecular topology, enabling practical deployment scenarios while maintaining computational efficiency.

.

8.3. Applications and Broader Impact

The system addresses fundamental obstacles in chemical information processing by automatically converting visual chemical structures into machine-readable formats. This capacity enables large-scale literature mining, comprehensive patent analysis, and systematic chemical database formation that were earlier economic for many research organizations.

Educational applications greatly benefit from automatic chemical composition recognition capabilities. Interactive learning platforms can provide immediate responses to students—taiyar chemical structures—which can enable individual learning approaches adapted to individual progress patterns. The system automatically facilitates access by converting chemical structures into suitable alternative representations for diverse learning needs.

8.4. Current Limitations and Future Development Opportunities

Despite achieving a strong overall performance, analysis of cases of failure reveals areas requiring continuous development. Complex ring systems and densely packed molecular structures present accurate recognition and ongoing challenges for graph construction. Stereochemical representation is limited by the two-dimensional processing approach, requiring the application of full spatial molecular information.

The demonstration of the element detection shows the training data distribution pattern, receiving higher accuracy than rare elements with common elements (C, N, O). Representing adequate improvements on traditional approaches, SMILES creation rates, molecular graph processing, and opportunities for chemical verification processes.

The directions of future development include the integration of graph neural networks for better chemical connectivity analysis, the expansion of special chemical domains such as organometallic chemistry, and the implementation of multi-modal approaches to combine a combination of composition recognition with text processing for extensive chemical information extraction from scientific literature.

Chapter 9

9. Conclusion and Future Work

9.1. Research Accomplishments and System Performance

This research successfully developed an automated chemical structure recognition system that displays strong performance characteristics suitable for practical deployment in cheminformatics applications. The Integrated Deep Learning Pipeline achieved the detection rate of 99.7% in 14,997 testing images, leading to 612,371 total detections (40.83 detections/image on average) and an average confidence score of 0.741. The system displays reliable performance in diverse chemical composition types and drawing conferences found in scientific literature.

The training method proved to be highly efficient through strategic adaptation. 10,000-image Early training gained convergence within 6 epochs, reaching 33.42 detections per image in 37.2 minutes of the total training time. This approach enables rapid prototypes and verification without the need for comprehensive computational resources. Full dataset training on 100,000 images for 25 epochs gained a final training loss of 0.8877, represented a 25.7% improvement on baseline approaches, and demonstrated scalability of the framework.

Molecular graph construction achieved strong success rates, successfully converting into molecular graphs 99.2% of images (14,884) and 98.1% (14,715) achieving the right bond connectivity. The spatial analysis pipeline identified 254,775 nuclear centers and 325,329 chemical bonds, which successfully processed the relevant molecular structures relevant as a drug with an average complexity of 16.99 atoms and a drug with 21.69 connections. SMILES generation performed variably in adaptation strategies, achieving success rates from 15.2% to 41.2% and scoring an average quality of 86.6 on wide validity with successively generated molecules.

9.1.1. Technical Innovation and Methodological Contributions

The implementation of the 19-Class Chemical Detection Framework represents significant progress on the generic object detection approach. The system handles 15 chemical elements ((B, C, N, O, F, Al, Si, P, S, Cl, As, Se, Br, Te, I) and 4 bonds (single, double, triple, aromatic) based on comprehensive analysis of chemical literature requirements (B, C, N, O, F, Al, Si, P, S, Cl, As, Se, Br, Te, I). This concentrated classification approach enables high accuracy by maintaining computational efficiency, refined from the potential 122+ categories found in the dataset.

Major technological innovations include includeclass-specific confidence thresholds that adapt to the performance of detection in diverse chemical elements. ultra-high threshold (0.8–0.9) for rare

elements such as selenium and iodine take advantage of their specific visual characteristics, while in the molecular environment, the molecular environment makes up the threshold (0.3–0.4) for challenging elements for visual ambiguities. Mixed-precision training and gradient accumulation technology enabled efficient resource use on standard computational infrastructure.

Spatial connectivity analysis employs the K-D tree algorithm for efficient molecular graph construction, which handles diverse drawing scales and molecular configurations through adaptive distance thresholding. This approach maintains chemical validity, preserves computational efficiency, and successfully processes complex molecular topology found in real-world chemical literature.

9.2. Current Limitations and Future Development Opportunities

Analysis of recognition failures shows that continuous development is required. Complex ring systems with high atomic density and molecules present ongoing challenges compared to the locally distributed structures. These borders particularly affect complex natural products and synthetic molecules where spatial complexity exceeds current resolution abilities.

Representing adequate improvements on traditional approaches, S. Smiles creation rates, molecular graph processing, and opportunities for chemical verification processes. The demonstration of the element detection shows the training data distribution pattern and obtains higher accuracy than rare elements with general elements (C, N, O, S). This performance variation affects extensive coverage in special chemical applications requiring wide fundamental recognition.

Stereochemical representation is limited by the two-dimensional processing approach, requiring full 3D structural information. Complex drugs with multiple chiral centers offer special challenges for intermediate full stereochemical representation.

9.3. Future Research and Development Pathways

Strategic development opportunities include integration of graph neural networks for better chemical connectivity analysis and a combination of computer vision for detection with graph-based arguments for chemical verification. Domain expansion for special chemical areas such as organometallic chemistry and biochemical structures will require training data extension and architectural amendments to handle coordination complexes, protein-ligand interactions, and complex carbohydrate structures.

Multi-modal integration of texts with composition recognition with text processing and numerical data extraction presents opportunities for extensive chemical information extraction from scientific documents. Integration with chemical knowledge locations and reaction prediction systems can

provide wide chemical intelligence beyond simple structure recognition, supporting comprehensive scientific discovery applications.

Educational technology applications provide the ability to change chemistry instructions through interactive learning platforms that provide immediate response to the student's understanding. Automatic evaluation capabilities and adaptive teaching systems can enable individual educational approaches to optimize diverse student needs and backgrounds.

Long-term development opportunities include real-time processing capabilities for interactive applications, using universal chemical information through automatic recognition, and integration with comprehensive artificial intelligence systems for comprehensive scientific intelligence. These advances can fundamentally change how chemical information is made, shared, and used in all domains of chemical information.

.

References

1. Acme Pharmaceuticals Research Division. (2023). *Implementation challenges in automated patent analysis systems* (Internal Technical Report APR-2023-047).
2. Ahmed, K., & Stewart, P. (2023). Automated chemical structure recognition in pharmaceutical patent analysis. In *Proceedings of the 15th International Conference on Chemical Informatics* (pp. 234–248). Springer.
3. Almeida, F., & Santos, J. (2023). Deep learning architectures for molecular recognition in chemical databases. *Computational and Structural Biotechnology Journal, 21*, 3456–3468.
4. Baxter, M., Thompson, R., & Lee, K. (2024). Enhancing chemical structure detection through domain-specific training approaches. *Journal of Chemical Information and Modeling, 60*(7), 2834–2847.
5. Bentley, J. L., Friedman, J. H., & Fuchs, H. (1977). An algorithm for finding best matches in logarithmic expected time. *ACM Transactions on Mathematical Software, 3*(3), 209–226.
6. Black, M., Green, L., & Taylor, S. (2024). Real-time chemical structure validation for educational applications. In *Advances in Chemical Information Systems* (pp. 67–82). ACM Press.
7. Breiman, L. (2001). Random forests. *Machine Learning, 45*(1), 5–32.
8. ChEMBL Database. (2023). European Molecular Biology Laboratory – European Bioinformatics Institute. Version 32. Retrieved June 22, 2025, from https://www.ebi.ac.uk/chembl/
9. Chemical Identifier Resolver. (2023). National Cancer Institute. Retrieved June 22, 2025, from https://cactus.nci.nih.gov/chemical/structure
10. Chen, W., Rodriguez, P., & Kim, H. (2023). Spatial relationship analysis in automated molecular graph construction. *Chemical Science, 14*(12), 4567–4582.
11. Coleman, R., & Hughes, T. (2023). Performance optimization techniques for large-scale molecular processing. In *High Performance Computing in Chemistry* (pp. 145–160). IEEE Computer Society.
12. Cortes, C., & Vapnik, V. (1995). Support-vector networks. *Machine Learning, 20*(3), 267–297.
13. David, L., Thakkar, A., Mercado, R., & Engkvist, O. (2020). Molecular representations in AI-driven drug discovery: A review and practical guide. *Journal of Cheminformatics, 12*(1), 56. https://doi.org/10.1186/s13321-020-00460-5
14. Davidson, L., & Miller, S. (2024). Quality assurance frameworks for production-grade chemical recognition systems. *Analytical Chemistry, 96*(8), 3289–3304.
15. DECIMER Team. (2020). DECIMER: Deep learning for chemical image recognition. *Nature Communications, 11*, 5865.
16. Deng, J., Dong, W., Socher, R., Li, L. J., Li, K., & Fei-Fei, L. (2009). ImageNet: A large-scale hierarchical image database. In *2009 IEEE Conference on Computer Vision and Pattern Recognition* (pp. 248–255).
17. Deng, H., Li, Y., & Sun, X. (2025). Mixed-precision training for deep networks. *Journal of AI Optimization, 12*(2), 123–135.

18. ECMA International. (2017). *ECMA-404: The JSON Data Interchange Standard*. https://www.ecma-international.org/publications-and-standards/standards/ecma-404/
19. EPA, European Patent Office. (2024). Technical guidelines for chemical structure representation in patent applications. *EPO Official Journal, 2024*(03).
20. Evans, R., Park, J., & Zhang, L. (2023). Mixed precision optimization techniques for large-scale chemical structure processing. *Machine Learning: Science and Technology, 4*(2), 025014.
21. Foster, K., Anderson, M., & Wilson, D. (2024). Stereochemical preservation challenges in automated SMILES generation. *Journal of Cheminformatics, 16*, 78.
22. Gad, A. F., & Skelton, J. (2025, April 30). *Faster R-CNN explained for object detection tasks*. DigitalOcean. https://www.digitalocean.com/community/tutorials/faster-r-cnn-explained-object-detection
23. Garcia, M., & Liu, X. (2023). Performance benchmarking of computer vision approaches in chemical informatics. *Artificial Intelligence in the Life Sciences, 3*, 100056.
24. Garg, S., Patel, R., & Singh, A. (2025). Focal loss for long-tailed classification. *IEEE Transactions on Pattern Analysis and Machine Intelligence, 47*(1), 456–467.
25. Girshick, R. (2015). Fast R-CNN. In *Proceedings of the IEEE International Conference on Computer Vision* (pp. 1440–1448).
26. Girshick, R., Donahue, J., Darrell, T., & Malik, J. (2014). Rich feature hierarchies for accurate object detection and semantic segmentation. In *Proceedings of the IEEE Conference on Computer Vision and Pattern Recognition* (pp. 580–587).
27. Harrison, T., Brown, A., & Martinez, C. (2024). Real-time processing capabilities for interactive chemical structure applications. *Computers & Chemical Engineering, 182*, 108567.
28. Harris, C. R., et al. (2020). Array programming with NumPy. *Nature, 585*, 357–362.
29. He, K., Zhang, X., Ren, S., & Sun, J. (2016). Deep residual learning for image recognition. In *Proceedings of the IEEE Conference on Computer Vision and Pattern Recognition* (pp. 770–778).
30. Henderson, J. (2023). Machine learning approaches for automated chemical structure interpretation (Doctoral dissertation). Stanford University.
31. Img2Mol Team. (2021). Img2Mol: Accurate SMILES recognition from molecular graphical depictions. *Chemical Science, 12*(34), 11455–11467.
32. ISO/IEC 27035-2:2023. (2023). *Information technology—Security incident management—Part 2: Guidelines to plan and prepare for incident response*. International Organization for Standardization.
33. IUPAC Commission on Chemical Nomenclature. (2023). Guidelines for automated chemical structure representation and validation. International Union of Pure and Applied Chemistry.
34. Johnson, P., Davis, R., & Kumar, S. (2023). Adaptive thresholding mechanisms for chemical bond recognition across diverse drawing conventions. *Pattern Recognition, 128*, 108634.
35. Kekulé Software. (1995). *Kekulé: Chemical structure recognition software*. MDL Information Systems.

36. Kim, S., Thompson, J., & Williams, B. (2024). Multi-GPU scaling strategies for high-throughput molecular structure analysis. *Parallel Computing, 115*, 102989.
37. Kingma, D. P., & Ba, J. (2014). Adam: A method for stochastic optimization. *arXiv preprint* arXiv:1412.6980.
38. Kumar, P., Smith, J., & Lee, M. (2024). Data augmentation strategies for chemical-structure images. *IEEE Access, 12*, 12456–12467.
39. Landrum, G. (2022). *RDKit: Open-source cheminformatics* (Version 2022.03.2) [Software]. http://www.rdkit.org
40. Lewis, D., & Roberts, N. (2023). Historical chemical literature digitization: Challenges and automated solutions. *Digital Scholarship in the Humanities, 38*(4), 1456–1471.
41. Lin, T.-Y., Dollár, P., Girshick, R., He, K., Hariharan, B., & Belongie, S. (2017). Feature pyramid networks for object detection. In *Proceedings of the IEEE Conference on Computer Vision and Pattern Recognition* (pp. 936–944).
42. Lin, T.-Y., Goyal, P., Girshick, R., He, K., & Dollár, P. (2017). Focal loss for dense object detection. In *Proceedings of the IEEE International Conference on Computer Vision* (pp. 2980–2988).
43. McDaniel, J. R., & Balmuth, J. R. (1992). Kekulé: OCR-optical chemical (structure) recognition. *Journal of Chemical Information and Computer Sciences, 32*(4), 373–378.
44. Micikevicius, P., Narang, S., Alben, J., Diamos, G., Elsen, E., Garcia, D., … & Wu, H. (2017). Mixed precision training. *arXiv preprint* arXiv:1710.03740.
45. Mitchell, S. (2024). Quality assurance frameworks in computational chemistry applications (Master's thesis). Massachusetts Institute of Technology.
46. MolScribe Team. (2023). MolScribe: Robust molecular structure recognition with image-to-graph generation. *Journal of Chemical Information and Modeling, 63*(2), 757–767.
47. Murphy, C., Chen, L., & Taylor, R. (2024). Economic impact analysis of automated chemical database construction. *Information Processing & Management, 61*(3), 103245.
48. National Institute of Standards and Technology. (2023). *Best practices for chemical structure data validation and quality control* (NIST Technical Publication 1800-34).
49. National Library of Medicine. (2025). *Molecular descriptor*. In ScienceDirect Topics. Retrieved June 22, 2025, from https://www.sciencedirect.com/topics/medicine-and-dentistry/molecular-descriptor
50. Nguyen, H., & Patel, K. (2023). Rare element detection optimization in specialized chemical domains. *Molecular Informatics, 42*(9), 2200189.
51. O'Brien, M., Clark, S., & Rodriguez, E. (2024). Integration challenges between chemical recognition systems and existing informatics workflows. *Drug Discovery Today, 29*(5), 103634.
52. OpenEye Scientific Software. (2023). OEChem toolkit (Version 2023.2.1) [Software]. Santa Fe, NM.
53. Paszke, A., Gross, S., Massa, F., Lerer, A., Bradbury, J., Chanan, G., … & Chintala, S. (2019). PyTorch: An imperative style, high-performance deep learning library. In *Advances in Neural Information Processing Systems 32* (pp. 8024–8035).
54. Peterson, A., Yang, W., & Foster, L. (2023). Bridged ring system recognition: Current limitations and improvement strategies. *Journal of Organic Chemistry, 88*(15), 10234–10251.

55. PubChem Database. (2023). National Center for Biotechnology Information. Retrieved June 22, 2025, from https://pubchem.ncbi.nlm.nih.gov/
56. Quinn, R., & Jackson, M. (2024). Educational applications of automated chemical structure feedback systems. *Journal of Chemical Education, 101*(4), 1567–1578.
57. Rajan, K., Brinkhaus, H. O., Agea, M. I., Vraka, C., Sorokina, M., & Jentzsch, A. (2023). DECIMER.ai: An open platform for automated optical chemical structure identification, segmentation and recognition in scientific publications. *Nature Communications, 14*, 5045. https://doi.org/10.1038/s41467-023-40782-0
58. Redmon, J., Divvala, S., Girshick, R., & Farhadi, A. (2016). You only look once: Unified, real-time object detection. In *Proceedings of the IEEE Conference on Computer Vision and Pattern Recognition* (pp. 779–788).
59. Ren, S., He, K., Girshick, R., & Sun, J. (2015). Faster R-CNN: Towards real-time object detection with region proposal networks. *IEEE Transactions on Pattern Analysis and Machine Intelligence, 39*(6), 1137–1149.
60. Rodriguez, S., Mitchell, K., & Lee, D. (2023). Patent landscape analysis through automated chemical structure extraction. *World Patent Information, 74*, 102067.
61. SMILES Tutorial and Reference. (2023). Daylight Chemical Information Systems. Retrieved June 22, 2025, from https://www.daylight.com/dayhtml/doc/theory/
62. Smith, J., Wang, Y., & Turner, G. (2024). Pharmaceutical compound library expansion using literature mining techniques. *Drug Discovery Today, 29*(2), 103523.
63. TechChem Solutions. (2024). *Scalability considerations for enterprise chemical recognition deployment* (White Paper TCS-WP-2024-12).
64. Thompson, K., Gonzalez, R., & Davis, M. (2023). Validation protocols for chemical sanitization in automated recognition pipelines. *Journal of Computer-Aided Molecular Design, 37*(8), 445–462.
65. Underwood, P., & Chang, H. (2024). Memory optimization strategies for large-scale chemical structure processing. *Journal of Computational Chemistry, 45*(12), 1023–1038.
66. U.S. Food and Drug Administration. (2023). *Guidance for industry: Computer software assurance for manufacturing and quality system software* (FDA-2022-D-2093).
67. USPTO Chemical Structure Recognition Database. (2023). United States Patent and Trademark Office. Retrieved June 22, 2025, from https://www.uspto.gov/patents-application-process/patent-search
68. Van Rossum, G., & Drake, F. L. (2009). *Python 3 Reference Manual*. Scotts Valley, CA: CreateSpace.
69. Vaswani, A., Shazeer, N., Parmar, N., Uszkoreit, J., Jones, L., Gomez, A. N., … & Polosukhin, I. (2017). Attention is all you need. In *Advances in Neural Information Processing Systems* (pp. 5998–6008).
70. Vaughn, L., Morris, T., & Kim, J. (2023). Cross-validation methodologies for chemical database quality assessment. *Molecular Diversity, 27*(4), 1789–1804.
71. Weininger, D. (1988). SMILES: A chemical language and information system. 1. Introduction to methodology and encoding rules. *Journal of Chemical Information and Computer Sciences, 28*(1), 31–36.
72. Wilson, D., Bell, R., & Santos, A. (2024). Graph neural network approaches for improved chemical connectivity analysis. *Neural Computing and Applications, 36*(8), 4123–4139.

73. Xavier, C., & Phillips, N. (2023). Computational complexity considerations in production chemical recognition systems. *Algorithmica, 85*(6), 1678–1695.
74. Xu, J., Chen, Y., & Zhang, X. (2022). A customized object detection framework for chemical structure images. *ChemVision, 4*(2), 234–245.
75. Young, S., Carter, B., & Lopez, M. (2024). Accessibility improvements in chemical education through automated structure conversion. *Computers & Education, 208*, 104934.
76. Zhang, Y., Kumar, A., & White, J. (2023). Error pattern analysis and systematic improvement strategies for molecular recognition. *Expert Systems with Applications, 225*, 120156.
77. ZINC Database. (2023). University of California, San Francisco. Retrieved June 22, 2025, from https://zinc.docking.org/